Physics Letters B 842 (2023) 137955

Contents lists available at ScienceDirect

Physics Letters B

journal homepage: www.elsevier.com/locate/physletb

Measurement of the $B_s^0 \to \mu^+\mu^-$ decay properties and search for the $B^0 \to \mu^+\mu^-$ decay in proton-proton collisions at $\sqrt{s} = 13\,\text{TeV}$

The CMS Collaboration *

CERN, Geneva, Switzerland

ARTICLE INFO

Article history:
Received 20 December 2022
Received in revised form 20 April 2023
Accepted 8 May 2023
Available online 12 May 2023
Editor: M. Doser

Dataset link: CMS data preservation, re-use and open access policy

Keywords:
CMS
BPH
Flavor physics
Rare decays

ABSTRACT

Measurements are presented of the $B_s^0 \to \mu^+\mu^-$ branching fraction and effective lifetime, as well as results of a search for the $B^0 \to \mu^+\mu^-$ decay in proton-proton collisions at $\sqrt{s} = 13\,\text{TeV}$ at the LHC. The analysis is based on data collected with the CMS detector in 2016–2018 corresponding to an integrated luminosity of $140\,\text{fb}^{-1}$. The branching fraction of the $B_s^0 \to \mu^+\mu^-$ decay and the effective B_s^0 meson lifetime are the most precise single measurements to date. No evidence for the $B^0 \to \mu^+\mu^-$ decay has been found. All results are found to be consistent with the standard model predictions and previous measurements.

1. Introduction

Rare B meson decays provide a sensitive probe for beyond-the-standard-model (BSM) effects and allow exploring energy scales much higher than the ones directly accessible at the CERN LHC. A key factor in the success of these studies is the availability of precise theoretical predictions for experimentally accessible processes. The leptonic decays $B_s^0 \to \mu^+\mu^-$ and $B^0 \to \mu^+\mu^-$ represent such a case, where precise theoretical predictions can be matched with a clear experimental signature. These rare decays are examples of flavor changing neutral current processes, which are strongly suppressed in the standard model (SM), making them sensitive to BSM physics contributions. In this Letter, when decays are mentioned, charge-conjugated decay modes are implied.

The $B_s^0 \to \mu^+\mu^-$ and $B^0 \to \mu^+\mu^-$ decays proceed through penguin and box diagrams that involve Z or W boson exchange and are furthermore helicity suppressed by a factor m_μ^2/m_B^2, where m_μ and m_B denote the masses of the muon and either the B_s^0 or B^0 meson. Moreover, the $B^0 \to \mu^+\mu^-$ decay is also Cabibbo–Kobayashi–Maskawa suppressed [1,2]. As a result, in the SM, the average time-integrated branching fractions for these decays are very small [3]:

$$\mathcal{B}(B_s^0 \to \mu^+\mu^-) = (3.66 \pm 0.14) \times 10^{-9},$$

$$\mathcal{B}(B^0 \to \mu^+\mu^-) = (1.03 \pm 0.05) \times 10^{-10}.$$

These predictions include next-to-leading order corrections of electroweak origin and next-to-next-to-leading order quantum chromodynamics (QCD) corrections. The largest contribution to the theoretical uncertainty is from the determining of the Cabibbo–Kobayashi–Maskawa matrix element values, in particular $|V_{cb}|$. The issue can be mitigated by considering a ratio of the branching fraction to the mass difference of the heavy and light B_s^0 and B^0 mesons [4].

A number of experiments at e^+e^- and hadron colliders have searched for these decays, but only recently the first observation of the $B_s^0 \to \mu^+\mu^-$ decay was reported in a combined analysis of data taken by the CMS and LHCb Collaborations [5], which was later confirmed by the ATLAS [6], CMS [7], and LHCb [8–10] experiments individually. Currently, the most precise measurement of the $B_s^0 \to \mu^+\mu^-$ branching fraction is achieved in a combined analysis of data from the three experiments [11]. The analysis shows a deviation from the SM prediction at the level of 2.4 standard deviations (σ) for the $B_s^0 \to \mu^+\mu^-$ branching fraction. No significant detection of the $B^0 \to \mu^+\mu^-$ decay has been reported so far.

A few recent measurements of the semileptonic $b \to s\ell^+\ell^-$ processes (where lepton $\ell = e$ or μ) have reported disagreements at the level of 2–3 σ with the SM predictions. Deviations were found in measurements of the differential branching fractions of the $B \to K^*\mu^+\mu^-$ and $B_s^0 \to \phi\mu^+\mu^-$ decays [12–15], angular observables in the $B \to K^*\mu^+\mu^-$ decays [16,17], and in searches for

* *E-mail address:* cms-publication-committee-chair@cern.ch.

https://doi.org/10.1016/j.physletb.2023.137955

lepton flavor universality violation via measurements of the R_K and R_{K^*} ratios [18–22]. Not all the individual measurements confirm these observations though [23,24] and the revised R_K and R_{K^*} measurements are found to be consistent with the SM [25,26].

In the framework of an effective field theory, the $b \to s\ell^+\ell^-$ decays are dominated by the semileptonic operators $O_9 = (\bar{s}_L\gamma_\mu b_L)(\bar{\ell}\gamma^\mu\ell)$ and $O_{10} = (\bar{s}_L\gamma_\mu b_L)(\bar{\ell}\gamma^\mu\gamma_5\ell)$. The BSM physics contributions could be observed as deviations of the corresponding Wilson coefficients (C_9 and C_{10}) from their SM values. As the $B_s^0 \to \mu^+\mu^-$ and $B^0 \to \mu^+\mu^-$ decays are dominated by the O_{10} operator, they may be sensitive to the same effects. In contrast to the semileptonic case, the nonperturbative hadronic contributions for leptonic B meson decays enter solely through decay constants f_B and f_{B_S}, which are precisely known from lattice QCD calculations [27], making the theory calculations more robust. Therefore, a precise measurement of the $B_s^0 \to \mu^+\mu^-$ decay properties may have a big impact on the interpretation of these anomalies.

The effective lifetime of the B_s^0 meson measured in the $B_s^0 \to \mu^+\mu^-$ decay is an independent and theoretically clean probe for BSM physics [28]. In the SM, the heavy ($B_{s,H}^0$) and light ($B_{s,L}^0$) mass eigenstates are linear combinations of the flavor eigenstates. The lifetimes of the heavy and light mass eigenstates are $\tau_H = 1.624 \pm 0.009$ ps and $\tau_L = 1.429 \pm 0.007$ ps, respectively [29]. Only the heavy $B_{s,H}^0$ mass eigenstate can decay to the $\mu^+\mu^-$ final state. This is because, in the absence of charge-conjugation and parity (CP) violation in the B_s^0 mixing, the B_s^0 mass eigenstates are also CP eigenstates, with the heavier one being CP odd, while $\mu^+\mu^-$ is also a CP-odd final state. Therefore, any significant deviation of the measurement from the established value for the $B_{s,H}^0$ lifetime would indicate a BSM physics contribution. Currently, the most precise measurement of the B_s^0 meson lifetime (τ) in the $B_s^0 \to \mu^+\mu^-$ decay, $\tau(B_s^0 \to \mu^+\mu^-) = 2.07 \pm 0.29$ ps, comes from the LHCb experiment [9,10].

In this Letter, we report on new measurements of the $B_s^0 \to \mu^+\mu^-$ decay properties and a search for the $B^0 \to \mu^+\mu^-$ decay based on proton-proton collision data collected by the CMS experiment in 2016–2018 at a center-of-mass energy of 13 TeV, corresponding to an integrated luminosity of 140 fb^{-1}. This new analysis uses improved techniques compared to the earlier publication based on 2011–2012 and 2016 data [7]; consequently the 2016 data sample has been re-analyzed, and the new results supersede the ones from Ref. [7]. Given that the sensitivity of the 2016–2018 data significantly exceeds that of the 2011–2012 sample, no attempt is made to combine the new results with those from 2011–2012 data. Tabulated results are provided in the HEPData record for this analysis [30].

2. Data analysis overview

The data analysis strategy employed in this measurement is based on the previous CMS studies of the $B_s^0 \to \mu^+\mu^-$ and $B^0 \to \mu^+\mu^-$ decays. We made several modifications and improvements to increase the analysis sensitivity, while also benefiting from the large amount of data collected in 2017–2018. Because of the increased sensitivity, new methods were developed to achieve a better understanding of various systematic effects.

Leptonic B meson decays are reconstructed by combining two oppositely charged muons, performing a common vertex fit, and imposing selection criteria to separate small signals from large backgrounds. Here and in what follows, we use the notation B to denote either the B^0 or B_s^0 meson. The dominant background sources are the combinatorial background where the two muons originate from two different heavy quarks, the partially reconstructed semileptonic decays where both muons originate from the same B meson, and the peaking background coming from the charmless two-body hadronic decays of B mesons.

The combinatorial and partially reconstructed backgrounds are the main limiting factors in the analysis sensitivity. Despite being reducible backgrounds with several distinct features, they are copious, which makes it difficult to reject them completely without losing a significant fraction of signal events. To maximize the analysis sensitivity, we perform a multivariate analysis (MVA) combining multiple discriminating observables in a single powerful discriminator (d_{MVA}) using a boosted decision tree algorithm. The training and performance evaluation of the MVA are described in Section 6.

The charmless two-body decays, such as $B^0 \to K^+\pi^-$ and $B_s^0 \to K^+K^-$, could mimic signal when both charged hadrons are misidentified as muons. We measure the misidentification probabilities in data using the $K_S^0 \to \pi^+\pi^-$, $\phi(1020) \to K^+K^-$, and $\Lambda \to p\pi^-$ decays after restricting the decay distance to match that of the B mesons. We find a reasonable agreement between the data and Monte Carlo (MC) simulation for pions and kaons, where the misidentification probability is dominated by pion and kaon decays to a muon and a muon antineutrino. The probability to misidentify protons as muons is an order of magnitude smaller according to simulation, and found to be even smaller in data, thus making contributions from the associated processes unimportant. With a stringent muon identification based on a multivariate analysis [7], we reduce the charmless two-body backgrounds to a negligible level compared to the dominant combinatorial background.

The results are extracted using simultaneous unbinned maximum likelihood (UML) fits in multiple categories (discussed in Section 7). For the branching fraction measurements, we perform a two-dimensional (2D) fit using the dimuon invariant mass ($m_{\mu^+\mu^-}$) and its uncertainty as the observables. For the lifetime extraction, we perform a three-dimensional (3D) fit using the dimuon mass, the decay time, and the decay time uncertainty as the observables.

Given the poor precision in the knowledge of the $b\bar{b}$ cross section at the LHC, a direct extraction of the branching fractions of the $B_s^0 \to \mu^+\mu^-$ and $B^0 \to \mu^+\mu^-$ decays would be affected by a large uncertainty. As commonly done in B physics analyses, the signal branching fraction is instead calculated by normalizing it to another decay channel of a B meson, for which the branching fraction is well known and whose characteristics allow for a precise reconstruction with small backgrounds. The $B^+ \to J/\psi K^+$ decay with $J/\psi \to \mu^+\mu^-$ is the best candidate in our case as a normalization channel. We also consider $B_s^0 \to J/\psi\phi(1020)$ decays with $\phi(1020) \to K^+K^-$ as a cross-check of the nominal result. The signal branching fractions $\mathcal{B}(B_s^0 \to \mu^+\mu^-)$ and $\mathcal{B}(B^0 \to \mu^+\mu^-)$ can then be extracted as

$$\mathcal{B}(B_s^0 \to \mu^+\mu^-) = \mathcal{B}(B^+ \to J/\psi K^+)\frac{N_{B_s^0\to\mu^+\mu^-}}{N_{B^+\to J/\psi K^+}} \times \frac{\varepsilon_{B^+\to J/\psi K^+}}{\varepsilon_{B_s^0\to\mu^+\mu^-}}\frac{f_u}{f_s}, \quad (1)$$

$$\mathcal{B}(B_s^0 \to \mu^+\mu^-) = \mathcal{B}(B_s^0 \to J/\psi\phi(1020))\frac{N_{B_s^0\to\mu^+\mu^-}}{N_{B_s^0\to J/\psi\phi(1020)}} \times \frac{\varepsilon_{B_s^0\to J/\psi\phi(1020)}}{\varepsilon_{B_s^0\to\mu^+\mu^-}}, \quad (2)$$

$$\mathcal{B}(B^0 \to \mu^+\mu^-) = \mathcal{B}(B^+ \to J/\psi K^+)\frac{N_{B^0\to\mu^+\mu^-}}{N_{B^+\to J/\psi K^+}} \times \frac{\varepsilon_{B^+\to J/\psi K^+}}{\varepsilon_{B^0\to\mu^+\mu^-}}\frac{f_u}{f_d}, \quad (3)$$

where N_X is the number of the candidates of decay X, as extracted from the fit, and ε_X is the corresponding full selection

efficiency derived from MC simulation. In addition, f_u, f_d, and f_s are the production fractions for B^+, B^0, and B_s^0 mesons, respectively. The ratio f_u/f_d is expected to be 1 in the SM due to isospin symmetry. The ratio f_s/f_u, as well as $\mathcal{B}(B^+ \to J/\psi K^+)$ and $\mathcal{B}(B_s^0 \to J/\psi\phi(1020))$, are external inputs discussed in Section 9.

Another advantage of measuring the branching fractions with respect to other decays is that it allows for a cancellation of many systematic uncertainties in the selection and reconstruction efficiencies of the signal and normalization channels.

To reduce unintentional bias, the analysis employs a "data blinding" technique. All optimization studies are performed using signal from MC simulation and background from data that does not include events with a dimuon mass of 5.15–5.50 GeV. Once the selection criteria and measurement procedure have been finalized, the data are unblinded.

3. The CMS detector

The central feature of the CMS apparatus is a superconducting solenoid of 6 m internal diameter, providing a magnetic field of 3.8 T. Within the solenoid volume are a silicon pixel and strip tracker, a lead tungstate crystal electromagnetic calorimeter, and a brass and scintillator hadron calorimeter, each composed of a barrel and two endcap sections. Forward calorimeters extend the pseudorapidity η coverage provided by the barrel and endcap detectors. Muons are measured in gas-ionization detectors embedded in the steel flux-return yoke outside the solenoid. A more detailed description of the CMS detector, together with a definition of the coordinate system used and the relevant kinematic variables, can be found in Ref. [31].

The silicon tracker used in 2016 measured charged particles within the range $|\eta| < 2.5$. For nonisolated particles with the transverse momentum of $1 < p_T < 10$ GeV and $|\eta| < 1.4$, the track resolutions were typically 1.5% in p_T and 25–90 (45–150) μm in the transverse (longitudinal) impact parameter [32]. At the start of 2017, a new pixel detector was installed [33]; the upgraded tracker measures particles up to $|\eta| = 3.0$ with typical resolutions of 1.5% in p_T and 20–75 μm in the transverse impact parameter [34] for nonisolated particles with $1 < p_T < 10$ GeV.

Muons are measured in the range $|\eta| < 2.4$, with detection planes made using three technologies: drift tubes, cathode strip chambers, and resistive-plate chambers. Matching muons to tracks measured in the silicon tracker results in a relative p_T resolution, for muons with p_T up to 100 GeV, of 1% in the barrel and 3% in the endcaps [35].

Events of interest are selected using a two-tiered trigger system. The first level, composed of custom hardware processors, uses information from the calorimeters and muon detectors to select events at a rate of around 100 kHz within a fixed latency of about 4 μs [36]. The second level, known as the high-level trigger, consists of a farm of processors running a version of the full event reconstruction software optimized for fast processing, and reduces the event rate to around 1 kHz before data storage [37].

4. Data and Monte Carlo simulation

We split the data collected with the CMS detector in 2016–2018 into four distinct periods: 2016a, 2016b, 2017, and 2018. The integrated luminosities of the corresponding samples are 20.0, 16.6, 42.0, and 61.3 fb^{-1} [38–40]. Data from the 2016a period were affected by strip tracker dynamic hit inefficiency. The problem was resolved in August 2016 and the rest of the 2016 data-taking period is referred to as 2016b. Before the 2017 data-taking period, the pixel detector was upgraded, improving the acceptance, redundancy, and resolution. During data taking in 2017, the pixel detector had synchronization issues at the beginning of the run, followed by DC-DC converter failures [33] leading to about 11% of the detector being unresponsive. Most of these issues were resolved before data taking began in 2018.

We use multiple samples of MC simulated events to evaluate the signal efficiency, the detector response, and the background yields. The simulated event samples are generated with PYTHIA 8.212 [41] using the CP5 underlying event tune [42] and propagated through the CMS detector model using the GEANT4 [43] package. The decays of B hadrons are simulated using the EVTGEN 1.3.0 [44] program and final-state photon radiation is described using PHOTOS 3.56 [45].

Multiple interactions within the same or nearby bunch crossings (pileup) are simulated for all samples by overlapping the hard-scattering event with several minimum bias events, with the multiplicity similar to the one observed in data (averaging to 23 for 2016 and 32 for 2017–2018).

5. Event reconstruction and selection

The events used in this analysis were collected with a set of dimuon triggers designed to select $B \to \mu^+\mu^-$, $B^+ \to J/\psi K^+$, and $B_s^0 \to J/\psi\phi(1020)$ events. To achieve an acceptable trigger rate, the first-level trigger required two high-quality [36] oppositely charged muons restricted to $|\eta| < 1.5$. At the high-level trigger, a high-quality dimuon secondary vertex (SV) [37] was required and the events were restricted to mass ranges of 4.5–6.0 GeV and 2.9–3.3 GeV for the B and J/ψ mesons, respectively. The J/ψ triggers additionally required the SV to be displaced from the beam spot (defined as the average interaction point in the plane transverse to the beams) and the displacement vector to be aligned with the dimuon momentum.

The event candidate selection starts with the reconstruction of dimuon candidates, which are used to build different B mesons for the signal and normalization channels. The selection is kept as similar as possible for all the channels to benefit from the cancellation of systematic effects in the ratio of the efficiencies used for the branching fraction normalization. Both muons are required to have a high-quality inner track [32] with $p_T > 4$ GeV and $|\eta| < 1.4$, and pass the tight muon identification requirements [7,35], which suppress misidentified muons from pion and kaon decays, and from other sources. Extra single and double kaons with $p_T > 1$ GeV and $|\eta| < 2.5$ are required for the $B^+ \to J/\psi K^+$ and $B_s^0 \to J/\psi\phi(1020)$ normalization channels, respectively.

We obtain B candidate properties by employing the kinematic fitter described in Ref. [46]. We apply different kinematic constraints depending on the final state. For the $B_s^0 \to \mu^+\mu^-$ and $B^0 \to \mu^+\mu^-$ decays, we use the vertex constraint, while for the $B^+ \to J/\psi K^+$ and $B_s^0 \to J/\psi\phi(1020)$ decays we also add a mass constraint for the J/ψ candidate.

From the B candidate's decay vertex and its momentum we build a refitted trajectory representing the B candidate. Then, for each reconstructed primary vertex (PV) in the event, the trajectory is extrapolated to the point closest to that vertex. The absolute distance between the closest point and the PV in 3D space is defined as the impact parameter. The PV with the smallest impact parameter is selected as the best PV for the B candidate.

Table 1 shows a summary of the B candidate selection requirements for the signal extraction and normalization UML fits. The 3D SV displacement significance is defined as the 3D distance between the PV and the dimuon SV, divided by its corresponding uncertainty. The 2D $\mu^+\mu^-$ pointing angle α is defined as the angle between the dimuon momentum and the line connecting the PV and SV, and is calculated in the transverse plane with respect to the beam direction. The pointing angle requirement is introduced to match the $\cos\alpha > 0.9$ requirement used in the J/ψ triggers.

Table 1
Selection requirements for the three decay channels used in the signal yield and normalization fits. Addition selection requirements are applied for the $B^+ \to J/\psi K^+$ control sample used in systematic studies.

Selection	$B \to \mu^+\mu^-$	$B^+ \to J/\psi K^+$	$B_s^0 \to J/\psi\phi(1020)$
B candidate mass [GeV]	[4.90, 5.90]	[4.90, 5.90]	[4.90, 5.90]
Blinding window [GeV]	[5.15, 5.50]		
$p_T(\mu)$ [GeV]	>4	>4	>4
$\lvert\eta(\mu)\rvert$	<1.4	<1.4	<1.4
3D SV displacement significance	>6	>4	>4
$\mu^+\mu^-$ p_T[GeV]	>5	>7	>7
$\mu^+\mu^-$ SV probability	>0.025	>0.1	>0.1
$\mu^+\mu^-$ invariant mass [GeV]		[2.9, 3.3]	[2.9, 3.3]
Kaon p_T[GeV]		>1	>1
J/ψ mass-constrained fit probability		>0.025	>0.025
2D $\mu^+\mu^-$ pointing angle [rad]		<0.4	<0.4
$\phi(1020)$ candidate mass [GeV]			[1.01, 1.03]
d_{MVA}	>0.9		

6. Multivariate analysis

Most of the observables used to distinguish signal from background have rather weak discriminating power. Therefore, we employ an MVA to combine them into a single, more powerful discriminator d_{MVA}. Compared to the previous analysis [7], we have relaxed the preselection requirements, developed new discriminating observables, added significantly more data for the model training, and used a more advanced machine learning algorithm. This allows us to significantly improve the analysis sensitivity, achieving the same level as in the previous measurement with just ∼60% of the previous data.

Inputs to the MVA are split into three major classes. The first class includes pointing angles, which are defined as the angles between the B candidate momentum and the line connecting the PV and SV, either in 2D or 3D. We use both definitions since the 2D version benefits from a smaller uncertainty in the vertex position and the 3D version provides additional matching information along the beam line. These observables are effective at rejecting all types of backgrounds, except for the ones originating from the two-body decays.

The second class of observables is related to the SV. The dimuon candidates from the combinatorial background tend to be associated with a low-quality SV fit. Therefore, the SV probability, calculated using the χ^2 and the number of degrees of freedom of the fit, is one of the most powerful discriminating variables. Furthermore, we achieve additional background suppression by rejecting events that contain a better-quality SV formed by one of the muons and any track in the event. Finally, most of the misreconstructed SVs tend to be close to the PV and therefore can be rejected using the SV displacement information.

The last class of observables is designed to detect nearby decay products present in semileptonic decays of b and c hadrons. We compute the number of tracks compatible with the $\mu^+\mu^-$ SV. In addition, isolation variables are calculated for the B candidate as well as both muon candidates. The isolation observables have been optimized in the previous studies [7] to maximize the separation power between the $B_s^0 \to \mu^+\mu^-$ signal and the background, while maintaining a reasonable agreement between the MC simulation and the data for the $B^+ \to J/\psi K^+$ normalization channel. The isolation is defined as

$$I = \frac{p_T}{p_T + \sum_{trk} p_T(trk)},$$

where p_T is the momentum of either the B or muon candidate and the sum includes all charged-particle tracks with $p_T > 0.9$ GeV in a cone of radius $\Delta R = \sqrt{(\Delta\eta)^2 + (\Delta\varphi)^2}$ around the candidate momentum direction, with φ representing the azimuthal angle in radians. Only the charged particles that do not belong to the candidate and are associated with the same PV are considered. The ΔR is required to be smaller than 0.7 for the B candidate isolation and 0.5 for the muon isolation.

For the MVA training, we employ the XGBoost library [47], which implements an advanced gradient boosting algorithm. The training is performed on a mixture of simulated $B_s^0 \to \mu^+\mu^-$ signal events and background events in data selected using the sidebands of the dimuon mass distribution consisting of two regions: 5.5–5.9 GeV populated by the combinatorial background and 4.9–5.1 GeV representing a combination of the partially reconstructed and combinatorial backgrounds. The events are split into training and testing categories in a 2:1 proportion. To reuse all available events, we train three classifiers by assigning events to one of the categories based on their event number modulo 3. This allows us to classify all events in data, making sure that no event was evaluated by a classifier that was trained on the event itself.

The $B^+ \to J/\psi K^+$ selection requirements in Table 1 define the *normalization* sample used to extract the final branching fractions. We also define a $B^+ \to J/\psi K^+$ *control* sample. This sample starts with an additional selection requirement of kaon $p_T < 1.5$ GeV, which effectively requires the kaon to carry only a small fraction of the parent B meson momentum, providing a better match with the $B \to \mu^+\mu^-$ kinematic distributions.

Even with the kaon $p_T < 1.5$ GeV requirement, there are still differences in the kinematic distributions for the two decays, which may have an impact on the analysis. The most important one is the difference in the invariant mass of the B_s^0 and J/ψ mesons, which has a significant impact on the opening angle between the two muons. The $J/\psi \to \mu^+\mu^-$ decay tends to have a larger uncertainty in the $\mu^+\mu^-$ vertex position along the dimuon momentum. Therefore the SV significance for the $B^+ \to J/\psi K^+$ events needs to be scaled by a factor of ∼1.6 to match the $B_s^0 \to \mu^+\mu^-$ distribution.

We use the $B^+ \to J/\psi K^+$ control sample to measure the MVA performance in data. To achieve the best matching between the d_{MVA} distributions for the $B_s^0 \to \mu^+\mu^-$ and $B^+ \to J/\psi K^+$ decays, we need to select appropriate input observables for the MVA in the $B^+ \to J/\psi K^+$ control sample. For the pointing angle and the impact parameter we use the $\mu^+\mu^-K^+$ final-state observables, since otherwise we would have an incorrect B candidate momentum vector. We also ignore the kaon track in all the isolation calculations and extra track counting. For the remaining inputs, we rely on the $\mu^+\mu^-$ observables only.

Fig. 1 shows a comparison of the d_{MVA} distributions for the $B^+ \to J/\psi K^+$ simulation and data. The data plots have backgrounds subtracted using the *sPlot* technique [48] applied to the UML fits of the $B^+ \to J/\psi K^+$ invariant mass distributions. We observe good agreement between the MC simulation and data for the 2016a and

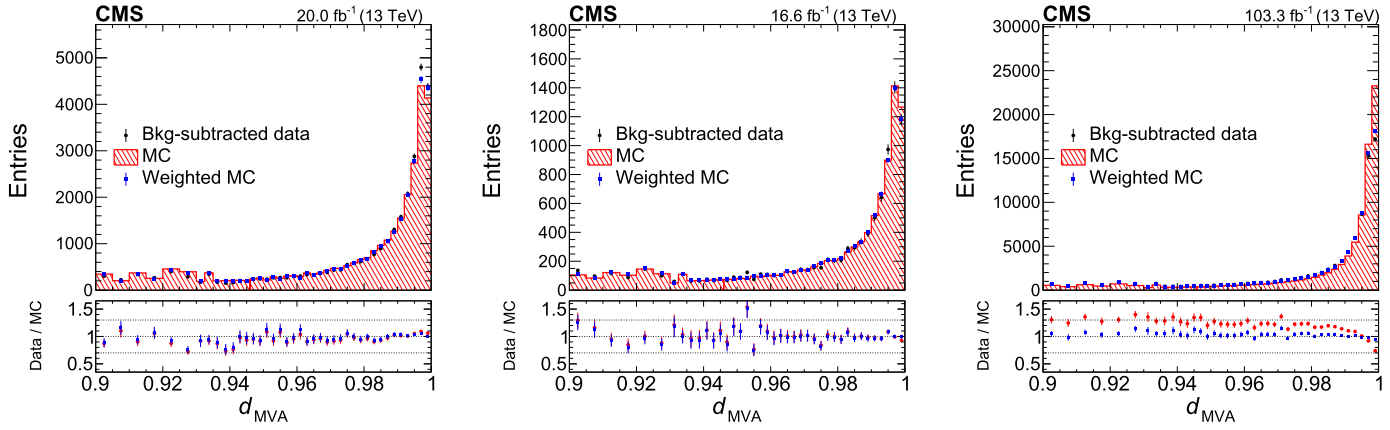

Fig. 1. Distributions of the d_{MVA} output for the 2016a (left), 2016b (center), and 2017–2018 (right) data and the corresponding MC samples. The blue squares represent the weighted simulated distributions using the XGBoost reweighting method. In the lower panel, the blue squares and red points are the ratio of the data to weighted and not weighted simulated distribution respectively. The MC distributions are normalized to the total number of events in data.

Table 2
Efficiency corrections for the $B_s^0 \to \mu^+\mu^-$ decays derived using two different methods: the efficiency ratio between data and simulation, and the XGBoost reweighting in $B^+ \to J/\psi K^+$ events. The quoted uncertainties are statistical only.

Method	$d_{MVA} > 0.9$ selection			$d_{MVA} > 0.99$ selection		
	2016	2017	2018	2016	2017	2018
Ratio	1.011 ± 0.013	0.939 ± 0.007	0.903 ± 0.008	1.058 ± 0.019	0.891 ± 0.008	0.885 ± 0.010
XGBoost	0.991 ± 0.008	0.949 ± 0.003	0.917 ± 0.002	1.008 ± 0.011	0.905 ± 0.004	0.908 ± 0.002

2016b samples. The agreement is worse for the 2017 and 2018 samples.

We derive corrections to the efficiency of the d_{MVA} selection requirements, defined in the caption of Table 2, in two different ways. The first ("Ratio") method derives the corrections using the $B^+ \to J/\psi K^+$ data and MC samples and applies them to the $B_s^0 \to \mu^+\mu^-$ and $B^0 \to \mu^+\mu^-$ efficiencies. The second ("XGBoost") method is based on the idea of reweighting the MC simulation samples to match the data. We were not able to find a single variable that would allow us to compensate for the discrepancy. Therefore we developed an approach using the XGBoost algorithm to train a classifier on the difference between the simulation and data in $B^+ \to J/\psi K^+$ events and use it to reweight the simulated $B \to \mu^+\mu^-$ events. We trained the XGBoost classifier using the same inputs that we use for the MVA. The backgrounds are subtracted from the data via the *sPlot* technique, as described above. The corrections from the two methods are summarized in Table 2. In general, the two methods give results compatible within $1–2\sigma$. We use the results from the XGBoost method as a default, and take the difference between the results of the two methods as a systematic uncertainty.

7. Data analysis

In order to extract results we perform a set of UML fits: the $B^+ \to J/\psi K^+$ and $B_s^0 \to J/\psi\phi(1020)$ yield fits, the simultaneous $B_s^0 \to \mu^+\mu^-$ and $B^0 \to \mu^+\mu^-$ branching fraction fit, and the $B_s^0 \to \mu^+\mu^-$ effective lifetime fit.

For the branching fraction measurement, we perform a 2D fit of the dimuon invariant mass and the relative mass resolution distributions within multiple event categories. The events are categorized using the following three independent criteria:

- data-taking period: 2016a, 2016b, 2017, or 2018,
- signal purity based on the d_{MVA} value: 0.90–0.99 or 0.99–1.00,
- $|\eta|$ of the most forward muon: 0.0–0.7 or 0.7–1.4,

leading to 16 distinct categories. The separation by $|\eta|$ of the most forward muon is motivated by different signal purities and mass resolutions in the two regions. The parameters of interest are the branching fractions of the $B_s^0 \to \mu^+\mu^-$ and $B^0 \to \mu^+\mu^-$ decays, which are derived from the corresponding yields.

The likelihood consists of five components: the B_s^0 signal, the B^0 signal, the partially reconstructed semileptonic background, the peaking $B \to h^+h^-$ background, where h represents a hadron, and the combinatorial background. The statistical uncertainties from the MC simulation and the systematic uncertainties are propagated to the final results by introducing nuisance parameters, which are profiled during the fit.

The signal components are modeled by Crystal Ball functions [49] and include the per-event mass resolution in the parameterization. The mass resolution and scale are calibrated using the $J/\psi \to \mu^+\mu^-$ and $\Upsilon(1S) \to \mu^+\mu^-$ data samples. All the parameters of the signal model are fixed in the fit, except for the width of the Crystal Ball function, which is a conditional parameter proportional to the dimuon mass resolution.

The semileptonic background is dominated by the three-body $B \to h^-\mu^+\nu$ and $B \to h\mu^+\mu^-$ processes. The contribution of this component is determined from the simulation of $B^0 \to \pi^-\mu^+\nu$, $B_s^0 \to K^-\mu^+\nu$, $B^+ \to \pi^+\mu^+\mu^-$, and $B^0 \to \pi^0\mu^+\mu^-$ decays. Contributions from $\Lambda_b \to p\mu^-\nu$ and $B_c^+ \to J/\psi\mu^+\nu$ backgrounds are found to be negligible compared with the uncertainty in the dominant background normalization. The shape of the semileptonic background is a Gaussian function with the mass and width parameters allowed to vary in the fit to the data.

The peaking $B \to h^+h^-$ background is represented by a sum of Gaussian and Crystal Ball functions with a common central mean value. The parameters used in the fit to the data are fixed from the results of a fit to the distribution obtained from MC simulation of $B^0 \to K^+K^-$, $K^+\pi^-$, $\pi^+\pi^-$, and $B_s^0 \to K^+K^-$, $K^-\pi^+$, $\pi^+\pi^-$ decays, with branching fractions from Ref. [29].

The yields of the semileptonic and peaking background components are calculated using the normalization channel and the corresponding MC simulation with the corrected efficiencies. Systematic uncertainties of 25% and 50% are assigned to the semileptonic

and peaking backgrounds, respectively, to account for uncertainties in the rate of misidentifying charged hadrons as muons. The nuisance parameters in the yield calculation, such as the ratio of the efficiencies and the normalization of the $B^+ \to J/\psi K^+$ process, are constrained using Gaussian or log-normal priors, according to the corresponding systematic uncertainties.

The combinatorial background is modeled by a linear function (constrained to be positive in the entire fit range). The yields and the slopes of the combinatorial background are free parameters in the UML.

We estimate the expected performance of the branching fraction measurement via an ensemble of pseudo-experiments generated using the SM values for the branching fractions and the lifetime. The relative uncertainties, which include the systematic uncertainties described in Section 8, are expected to be $^{+11.1}_{-10.5}$ % in $\mathcal{B}(B_s^0 \to \mu^+\mu^-)$ and $^{+67}_{-62}$ % in $\mathcal{B}(B^0 \to \mu^+\mu^-)$.

To extract the effective lifetime of the B_s^0 meson in the $B_s^0 \to \mu^+\mu^-$ decay, we perform a 3D UML fit to the dimuon invariant mass, decay time, and decay time uncertainty, dividing the data by data-taking period, d_{MVA} value, and rapidity of the most forward muon, as we do for the branching fraction fit. The signal acceptance as a function of the decay time is extracted from simulation and corrected with the $B^+ \to J/\psi K^+$ decays in data. To minimize the differences between the two channels, we use the $B^+ \to J/\psi K^+$ control sample defined in Section 6, along with its MVA. The combinatorial background decay time distribution was obtained from a mass sideband in data. The decay time uncertainty is calculated for each event and is used as an observable in the fit. The decay time uncertainty models are obtained from the simulation samples and sideband data. Using pseudo-experiments generated with a complete $B_s^0 \to \mu^+\mu^-$ model, the expected total uncertainty in the lifetime is found to be $^{+0.18}_{-0.16}$ ps.

8. Systematic uncertainties

8.1. Branching fraction measurement

The branching fraction measurements have multiple sources of experimental and theoretical systematic uncertainties. The experimental uncertainties are dominated by the uncertainty in the $B \to \mu^+\mu^-$ signal efficiency corrections due to mismodeling of d_{MVA} in MC simulation, the kaon reconstruction and selection efficiency for the $B^+ \to J/\psi K^+$ and $B_s^0 \to J/\psi\phi(1020)$ normalization measurements, and the trigger efficiency difference between the signal and normalization channels. The uncertainties in the branching fractions of the $B^+ \to J/\psi K^+$ and $B_s^0 \to J/\psi\phi(1020)$ decays, as well as in f_s/f_u, are considered to be external uncertainties, which are factorized out in the final results.

The signal efficiency corrections for mismodeling of the d_{MVA} distribution are estimated with two different methods described in Section 6. The two methods give results compatible with each other. Based on the difference between the two methods, we assign a 2 (3)% systematic uncertainty in the corrections for the $B_s^0 \to \mu^+\mu^-$ and $B^0 \to \mu^+\mu^-$ signal efficiencies for the $d_{MVA} > 0.90$ (0.99) selection ("d_{MVA} correction").

The hadron tracking efficiency uncertainty is obtained by comparing the ratio of the measured branching fractions of the two-body $D^0 \to K^-\pi^+$ to the four-body $D^0 \to K^-\pi^+\pi^+\pi^-$ decays to the world average value [29]. This gives a "Tracking efficiency" uncertainty of 2.3% [50] for each kaon.

As a result of the different kinematics and triggers for the signal and normalization channels, the trigger efficiency effects do not fully cancel and are corrected using MC simulation. The simulation of the trigger efficiency is checked by comparing with the efficiency measured using data obtained from other triggers. The observed differences between simulation and data are used to establish a "Trigger efficiency" systematic uncertainty of 3.7 (2.4)% for 2016 (2017–2018).

Table 3
Summary of the systematic uncertainties for the $B_s^0 \to \mu^+\mu^-$ and $B^0 \to \mu^+\mu^-$ branching fraction measurements.

Effect	$B_s^0 \to \mu^+\mu^-$	$B^0 \to \mu^+\mu^-$
f_s/f_u ratio of the B meson production fractions	3.5%	–
d_{MVA} correction	2–3%	
Tracking efficiency (per kaon)	2.3%	
Trigger efficiency	2.4–3.7%	
Fit bias	2.2%	4.5%
Pileup	1%	
Vertex quality requirement	1%	
$B^+ \to J/\psi K^+$ shape uncertainty	1%	
$B^+ \to J/\psi K^+$ branching fraction	1.9%	

There are a few more systematic uncertainties in the measurement. The fit bias is extracted from the difference between the branching fraction obtained from the pseudo-experiments and the input SM value, combined with the variation caused by using different background models in the fit ("Fit bias"). The shape uncertainty in the normalization channel is derived by using different signal templates in the yield fits ("$B^+ \to J/\psi K^+$ shape uncertainty"). The pileup uncertainty is extracted from the difference in the efficiency performance derived using the pileup distribution in data and in MC simulation ("Pileup"). The normalization channels use a tighter SV probability requirement than the signal channel because of the different triggers. The corresponding uncertainty is evaluated by comparing the efficiency difference between the tighter and the signal channel SV probability requirement (>0.100 with respect to >0.025) in the data and MC simulation in $B^+ \to J/\psi K^+$ events ("Vertex quality requirement"), where the data is from a sample that is triggered without the SV probability requirement.

Table 3 summarizes the systematic uncertainties for the branching fraction measurements using $B^+ \to J/\psi K^+$ events for normalization, including the $B^+ \to J/\psi K^+$ branching fraction uncertainty [29]. For the $B_s^0 \to \mu^+\mu^-$ branching fraction measurement with the $B_s^0 \to J/\psi\phi(1020)$ normalization, the systematic uncertainty in the tracking efficiency is doubled to 4.6% due to the presence of two kaons in the final state, and the shape uncertainty is found to be 1.5%. At the same time, this measurement could be free from explicitly taking into account the B production fraction systematic uncertainty, as discussed in Section 9.

The lifetime of the B_s^0 meson has a significant impact on the signal efficiency for the $B_s^0 \to \mu^+\mu^-$ decays. The branching fraction measurements are reported assuming the SM value for the lifetime (1.61 ps). Since the lifetime affects the branching fraction measurements, we provide a correction for alternative lifetime hypotheses. The scale factor for the branching fraction is $1.577 - 0.358\tau$, where τ is the B_s^0 meson lifetime in ps.

8.2. Lifetime measurement

The dominant source of systematic uncertainty in the lifetime measurement is associated with mismodeling of the correlation between the d_{MVA} and the decay time. This correlation stems from the most discriminating MVA variables, the pointing angle and its uncertainty, both of which are strongly correlated with the decay time. The correlation enters via the decay distance: the larger the decay distance is, the better one knows the direction from the PV to SV. As the decay distance gets shorter, the uncertainty in the pointing angle increases, making such events harder to distinguish from the background. Mismodeling of these correlations in simulation can have a significant impact on the decay time distribution.

Table 4
Summary of the systematic uncertainties in the $B_s^0 \to \mu^+\mu^-$ effective lifetime measurement (in ps) in four data-taking periods.

Effect	2016a	2016b	2017	2018
Lifetime fit bias	0.04	0.04	0.05	0.04
Decay time distribution mismodeling	0.10	0.06	0.02	0.02
Efficiency modeling		0.01		
Lifetime dependence		0.01		
Total	0.11	0.07	0.05	0.04

The decay time is also correlated with many selection requirements. Most of them are well simulated. We measure the lifetime bias in $B^+ \to J/\psi K^+$ events using a relaxed selection requirement, $d_{MVA} > 0.90$, and compare it to the prediction from simulation. We find the bias for the lifetime measurement to be 0.04–0.05 ps, depending on the data-taking period ("Lifetime fit bias").

For the final selection, we derive a correction as a ratio of the decay time distributions for the $d_{MVA} > 0.99$ and $d_{MVA} > 0.90$ requirements using $B^+ \to J/\psi K^+$ events in data. Then we apply this correction to the $B_s^0 \to \mu^+\mu^-$ decay time distribution extracted from simulation using $d_{MVA} > 0.90$ as the selection requirement. Repeating the procedure using simulated events, we find that the method may introduce a bias of up to 0.10 ps in 2016 data. The bias is found to be much smaller in 2017 and 2018 data. These effects ("Decay time distribution mismodeling") are taken into account in the lifetime fit by introducing independent nuisance parameters in the fit model.

Two additional minor systematic uncertainties are also included. The uncertainty from the imperfect parameterization of the efficiency dependence on the decay time is derived using different analytical functions in the lifetime fit to $B^+ \to J/\psi K^+$ events ("Efficiency modeling"). We also measure the lifetime in the MC samples generated with different lifetimes from the pseudo-experiments while sharing the same efficiency function. The difference between the measured lifetime and the input lifetime of the MC samples is assigned as a systematic uncertainty ("lifetime dependence").

Table 4 summarizes the systematic uncertainties in the lifetime measurement. The uncertainties of 2017 and 2018 data-taking periods are treated as correlated and other two are treated as uncorrelated.

9. Results

Using the result of the $B^+ \to J/\psi K^+$ normalization fit with Eqs. (1) and (3), we find the branching fractions to be:

$$\mathcal{B}(B_s^0 \to \mu^+\mu^-) = \\ = \left[3.83^{+0.38}_{-0.36}\,(\text{stat})^{+0.19}_{-0.16}(\text{syst})^{+0.14}_{-0.13}\,(f_s/f_u)\right] \times 10^{-9},$$

$$\mathcal{B}(B^0 \to \mu^+\mu^-) = \left[0.37^{+0.75}_{-0.67}\,(\text{stat})^{+0.08}_{-0.09}(\text{syst})\right] \times 10^{-10}.$$

The correlation between the extracted $\mathcal{B}(B_s^0 \to \mu^+\mu^-)$ and $\mathcal{B}(B^0 \to \mu^+\mu^-)$ branching fractions is -0.120. These results are based on the following external inputs:

- $\mathcal{B}(B^+ \to J/\psi K^+) = (1.020 \pm 0.019) \times 10^{-3}$,
- $\mathcal{B}(J/\psi \to \mu^+\mu^-) = (5.961 \pm 0.033) \times 10^{-2}$, and
- $f_s/f_u = 0.231 \pm 0.008$.

The branching fractions are taken from Ref. [29]. The f_s/f_u ratio is derived from the p_T-dependent measurement of the f_s/f_u ratio by LHCb [51]. We are using the p_T distribution observed in this measurement, shown in Fig. 2, to compute an effective f_s/f_u ratio

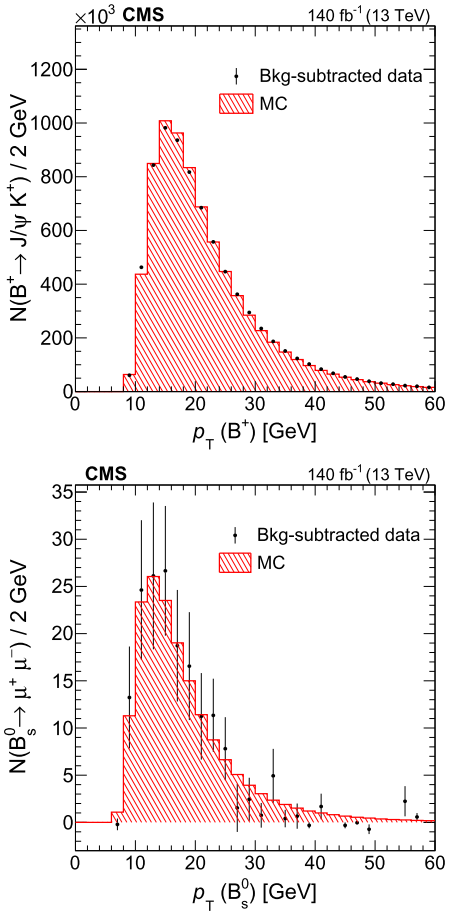

Fig. 2. The distribution of the B meson p_T after the *sPlot* background subtraction in data (points with error bars) and simulation (hatched histogram) for $B^+ \to J/\psi K^+$ (upper) and $B_s^0 \to \mu^+\mu^-$ (lower) events. The MC distributions are normalized to the total number of events in data.

for the corresponding phase space. Measurements of the p_T and η dependence of the ratio by the CMS Collaboration [52] are found to be consistent with the LHCb results.

The mass projections of the likelihood fits with all four data-taking periods combined together are shown in Fig. 3. The event yields for each component of the fit are summarized in Table 5. The profile likelihood as a function of the $B_s^0 \to \mu^+\mu^-$ and $B^0 \to \mu^+\mu^-$ branching fractions for 1D and 2D cases are shown in Fig. 4.

We also estimate the branching fractions using the $B_s^0 \to J/\psi\phi(1020)$ decays for the normalization. While this result is free from the explicit systematic uncertainty in the f_s/f_u ratio, it depends on the $B_s^0 \to J/\psi\phi(1020)$ branching fraction. At the moment, this branching fraction measurement uses the f_s/f_u ratio measurement as an input, but this dependence may be eliminated when new independent measurements of the $B_s^0 \to J/\psi\phi(1020)$ branching fraction become available, such as the measurement planned by the Belle II Collaboration at the KEKB e^+e^- collider [53] using the $\Upsilon(5S)$ data. Experimentally, the measurement based on the $B_s^0 \to J/\psi\phi(1020)$ normalization channel has slightly larger systematic uncertainties due to the presence of the second kaon in the final state.

Taking the world average value of $\mathcal{B}(B_s^0 \to J/\psi\phi(1020)) = (1.04 \pm 0.040) \times 10^{-3}$ [29], dominated by the LHCb measurement [51], and using the result of the $B_s^0 \to J/\psi\phi(1020)$ normalization fit with Eq. (2), we get:

$$\mathcal{B}(B_s^0 \to \mu^+\mu^-) =$$

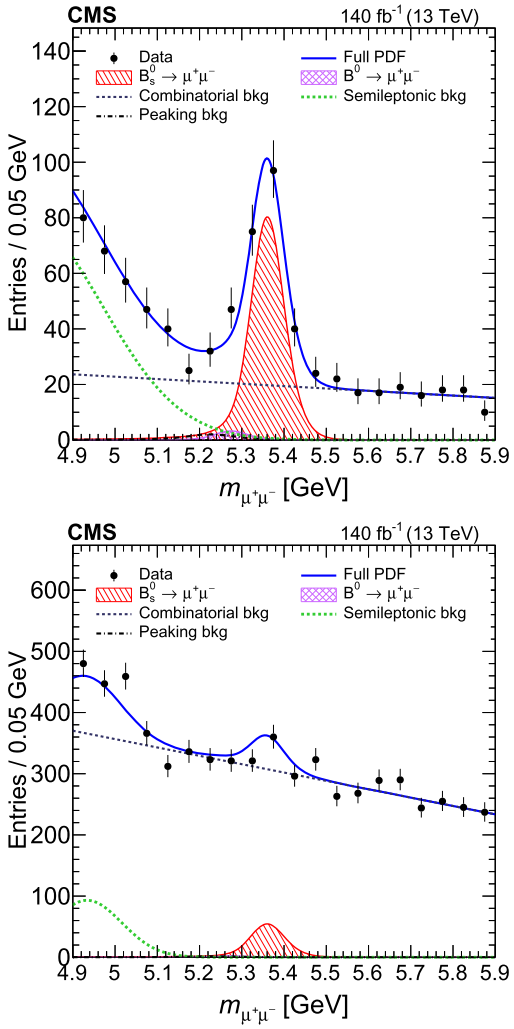

Fig. 3. The projections on the dimuon mass axis of the fit to the branching fraction for the $d_{\mathrm{MVA}} > 0.99$ (upper) and $0.99 > d_{\mathrm{MVA}} > 0.90$ (lower) categories. The solid blue curves represent the corresponding projections of the final fit model, while the individual components of the fit are represented by the dashed curves (backgrounds) and hatched histograms (signals).

$$= \left[4.02^{+0.40}_{-0.38}\,(\mathrm{stat})^{+0.28}_{-0.23}\,(\mathrm{syst})^{+0.18}_{-0.15}\,(\mathcal{B})\right] \times 10^{-9},$$

where the last uncertainty comes from the uncertainty in the $\mathrm{B}^0_\mathrm{s} \to \mathrm{J}/\psi\phi(1020)$ branching fraction.

The 90 and 95% confidence level (CL) upper limits on $\mathcal{B}(\mathrm{B}^0 \to \mu^+\mu^-)$ are evaluated using the $\mathrm{CL_s}$ criterion [54,55] and found to be

$$\mathcal{B}(\mathrm{B}^0 \to \mu^+\mu^-) < 1.5 \times 10^{-10} \text{ at } 90\%\ \mathrm{CL},$$

$$\mathcal{B}(\mathrm{B}^0 \to \mu^+\mu^-) < 1.9 \times 10^{-10} \text{ at } 95\%\ \mathrm{CL},$$

as shown in Fig. 5.

The effective lifetime for the $\mathrm{B}^0_\mathrm{s} \to \mu^+\mu^-$ decay is found to be

$$\tau = 1.83^{+0.23}_{-0.20}\,(\mathrm{stat})^{+0.04}_{-0.04}\,(\mathrm{syst})\,\mathrm{ps}.$$

The UML fit projection on the decay time axis for the signal region $5.28 < m_{\mu^+\mu^-} < 5.48\,\mathrm{GeV}$ is shown in Fig. 6. The observed lifetime is consistent with the world average value of $1.624 \pm 0.009\,\mathrm{ps}$ [29] within $1\,\sigma$, and therefore we do not correct the corresponding selection efficiency when performing the branching fraction measurement.

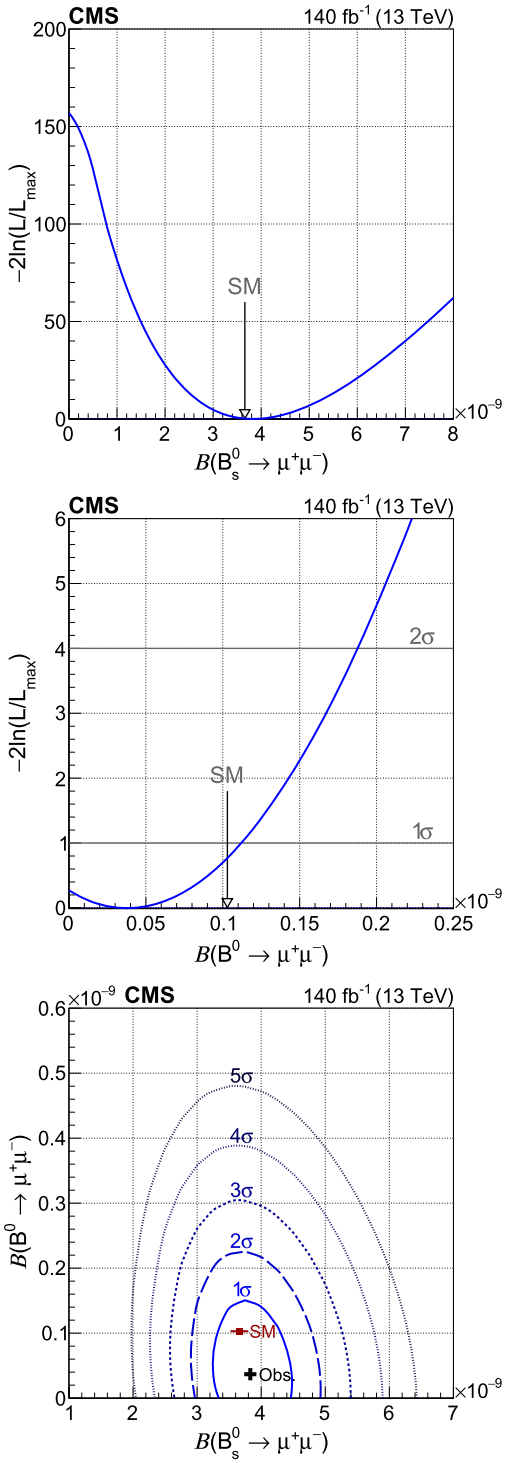

Fig. 4. The profile likelihood as a function of $\mathrm{B}^0_\mathrm{s} \to \mu^+\mu^-$ (upper) and $\mathrm{B}^0 \to \mu^+\mu^-$ (middle) decay branching fractions in 1D (top and middle plots) and in 2D (lower plot). The contours in 2D enclose the regions with 1–5 σ coverage, where 1, 2, and 3 σ regions correspond to 68.3, 95.4, and 99.7% confidence levels, respectively.

10. Summary

Measurements of the branching fraction ($\mathcal{B}$) of the $\mathrm{B}^0_\mathrm{s} \to \mu^+\mu^-$ decay and the effective B^0_s meson lifetime in this decay based on a data set of proton-proton collisions at $\sqrt{s} = 13\,\mathrm{TeV}$ corresponding to an integrated luminosity of $140\,\mathrm{fb}^{-1}$ have been presented and found to be:

Table 5
The expected event yields for $B_s^0 \to \mu^+\mu^-$ ($N(B_s^0)$), $B^0 \to \mu^+\mu^-$ ($N(B^0)$), the combinatorial background (N(comb)), the peaking background (N(peak)), and the semileptonic background (N(semi)) are summarized for each category (post-fit). The total expected and observed event yields are given in N(total) and Data column, respectively. Regions 0 and 1 refer to the ranges of 0.0–0.7 and 0.7–1.4, respectively, for the $|\eta|$ of the most forward muon. The uncertainties are statistical only.

Data set	Region	$N(B_s^0)$	$N(B^0)$	N(comb)	N(peak)	N(semi)	N(total)	Data
$d_{MVA} > 0.99$								
2016a	0	5.3 ± 0.6	0.2 ± 0.4	2.8 ± 1.9	0.2 ± 0.1	5.9 ± 1.2	14.5 ± 2.3	16
2016a	1	9.4 ± 1.0	0.4 ± 0.7	16.3 ± 5.6	0.4 ± 0.2	9.8 ± 1.9	36.2 ± 5.4	35
2016b	0	6.3 ± 0.7	0.3 ± 0.5	1.8 ± 2.0	0.2 ± 0.1	7.8 ± 1.5	16.3 ± 2.8	12
2016b	1	9.9 ± 1.1	0.4 ± 0.8	8.7 ± 5.6	0.4 ± 0.2	13.1 ± 2.5	32.5 ± 5.1	32
2017	0	23.5 ± 2.5	1.0 ± 1.9	51.7 ± 11.0	0.7 ± 0.3	29.3 ± 4.9	106.2 ± 9.8	114
2017	1	33.8 ± 3.5	1.4 ± 2.7	90.1 ± 14.0	1.4 ± 0.5	43.5 ± 6.9	170.1 ± 12.3	165
2018	0	34.4 ± 3.6	1.4 ± 2.8	65.1 ± 12.5	1.3 ± 0.5	38.1 ± 6.0	140.2 ± 11.1	143
2018	1	49.9 ± 5.2	2.0 ± 4.0	151.6 ± 17.5	2.4 ± 1.0	50.5 ± 7.8	256.4 ± 15.4	252
$0.99 > d_{MVA} > 0.90$								
2016a	0	4.8 ± 0.5	0.2 ± 0.4	118.1 ± 11.6	0.2 ± 0.1	8.3 ± 1.8	131.6 ± 11.4	132
2016a	1	8.9 ± 1.0	0.4 ± 0.7	325.1 ± 19.1	0.4 ± 0.2	16.3 ± 3.3	351.0 ± 18.7	352
2016b	0	5.5 ± 0.6	0.2 ± 0.5	107.9 ± 11.4	0.2 ± 0.1	10.7 ± 2.2	124.5 ± 11.1	126
2016b	1	9.2 ± 1.0	0.4 ± 0.7	257.4 ± 17.3	0.4 ± 0.2	18.0 ± 3.5	285.4 ± 16.9	287
2017	0	15.1 ± 1.8	0.6 ± 1.2	638.2 ± 26.6	0.7 ± 0.3	26.1 ± 4.7	680.7 ± 26.1	683
2017	1	21.6 ± 2.5	0.9 ± 1.8	1431.2 ± 39.6	1.0 ± 0.4	43.7 ± 7.8	1498.5 ± 38.7	1498
2018	0	23.2 ± 2.7	1.0 ± 1.9	937.3 ± 33.6	1.1 ± 0.5	51.5 ± 9.9	1014.2 ± 31.8	1017
2018	1	34.1 ± 4.0	1.4 ± 2.8	2223.5 ± 50.6	1.8 ± 0.7	78.7 ± 14.0	2339.5 ± 48.3	2340

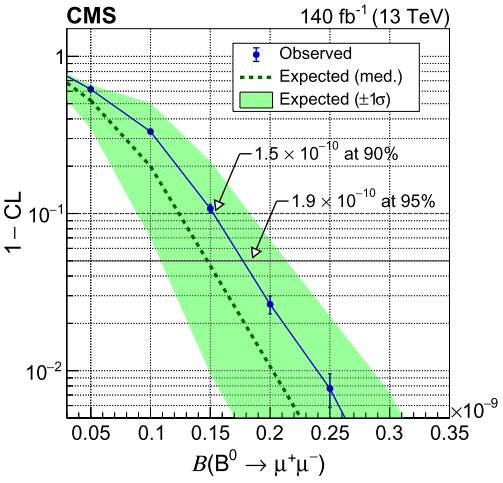

Fig. 5. The upper limits on the $B^0 \to \mu^+\mu^-$ decay branching fraction using the CL_s method. The dashed line represents the expected median value of the quantity $1 - CL$ for the background-only hypothesis, while the solid line shows the observed value. The shaded region indicates the $\pm 1\sigma$ band.

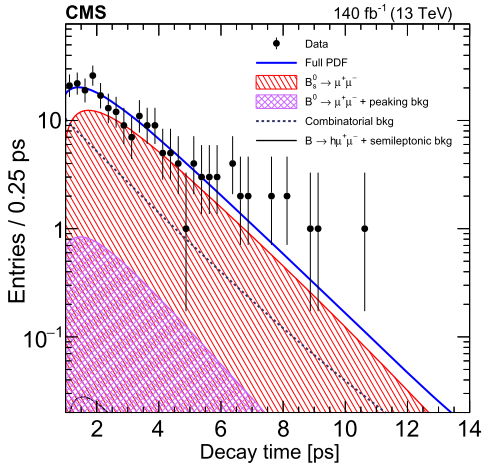

Fig. 6. The UML fit projection on the decay time axis for the signal region $5.28 < m_{\mu^+\mu^-} < 5.48$ GeV.

$$\mathcal{B}(B_s^0 \to \mu^+\mu^-) = \\ = \left[3.83^{+0.38}_{-0.36}\,(\text{stat})^{+0.19}_{-0.16}\,(\text{syst})^{+0.14}_{-0.13}\,(f_s/f_u)\right] \times 10^{-9},$$

$$\tau = 1.83^{+0.23}_{-0.20}\,(\text{stat})^{+0.04}_{-0.04}\,(\text{syst})\,\text{ps}.$$

Both measurements are the most precise single measurements to date and consistent with the standard model (SM) predictions and previous measurements within one standard deviation. The relative total uncertainty in $\mathcal{B}$ is reduced from 23 to 11% compared with the previous CMS measurement [7], based on 2011-2012 and partial 13 TeV data sets, while the central value is found to be somewhat higher. The 2016 data sample has been re-analyzed and the new results supersede the ones from Ref. [7]. The new analysis applied to the 2016 data yields a central value similar to the original measurement, indicating that the shift in the central value is driven mostly by the new data.

The search for the $B^0 \to \mu^+\mu^-$ decay has not revealed a significant event excess with respect to the dominant combinatorial background prediction. The 95% confidence level upper limit on the branching fraction is found to be

$$\mathcal{B}(B^0 \to \mu^+\mu^-) < 1.9 \times 10^{-10} \text{ at } 95\%\text{ CL}.$$

More data will be required to establish its existence and compare the result with the SM predictions.

Compared with the latest LHCb measurement [9,10]

$$\mathcal{B}(B_s^0 \to \mu^+\mu^-) = (3.09^{+0.46}_{-0.43}\,(\text{stat})^{+0.15}_{-0.11}\,(\text{syst})) \times 10^{-9},$$

our result with the combined systematic uncertainty including the external uncertainties, is about 1.2 standard deviations higher. These two measurements will shift the world average from its current value of $\mathcal{B}(B_s^0 \to \mu^+\mu^-) = (2.69^{+0.37}_{-0.35}) \times 10^{-9}$ [11] to a larger value, more consistent with the SM prediction, thus reducing the overall tension. The new measurement of the $B_s^0 \to \mu^+\mu^-$ branching fraction is an important input to the global fits to the flavor data (e.g., Ref. [56]) in light of the reported $b \to s\ell^+\ell^-$ anomalies (where lepton $\ell = e$ or μ).

The uncertainties in the branching fraction and effective lifetime measurements are dominated by the statistical component, which means that significant improvements can be expected in the precision of future measurements with the LHC Run 3 data.

The effective B_s^0 meson lifetime measurement in the $B_s^0 \to \mu^+\mu^-$ decay has achieved a precision comparable with the lifetime

difference between the heavy and light B_s^0 meson mass eigenstates, thus offering sensitivity to potential beyond-the-SM physics effects in the effective lifetime.

Declaration of competing interest

The authors declare that they have no known competing financial interests or personal relationships that could have appeared to influence the work reported in this paper.

Data availability

Release and preservation of data used by the CMS Collaboration as the basis for publications is guided by the CMS policy as stated in "CMS data preservation, re-use and open access policy".

Acknowledgements

We congratulate our colleagues in the CERN accelerator departments for the excellent performance of the LHC and thank the technical and administrative staffs at CERN and at other CMS institutes for their contributions to the success of the CMS effort. In addition, we gratefully acknowledge the computing centers and personnel of the Worldwide LHC Computing Grid and other centers for delivering so effectively the computing infrastructure essential to our analyses. Finally, we acknowledge the enduring support for the construction and operation of the LHC, the CMS detector, and the supporting computing infrastructure provided by the following funding agencies: BMBWF and FWF (Austria); FNRS and FWO (Belgium); CNPq, CAPES, FAPERJ, FAPERGS, and FAPESP (Brazil); MES and BNSF (Bulgaria); CERN; CAS, MOST, and NSFC (China); MINCIENCIAS (Colombia); MSES and CSF (Croatia); RIF (Cyprus); SENESCYT (Ecuador); MoER, ERC PUT and ERDF (Estonia); Academy of Finland, MEC, and HIP (Finland); CEA and CNRS/IN2P3 (France); BMBF, DFG, and HGF (Germany); GSRI (Greece); NKFIH (Hungary); DAE and DST (India); IPM (Iran); SFI (Ireland); INFN (Italy); MSIP and NRF (Republic of Korea); MES (Latvia); LAS (Lithuania); MOE and UM (Malaysia); BUAP, CINVESTAV, CONACYT, LNS, SEP, and UASLP-FAI (Mexico); MOS (Montenegro); MBIE (New Zealand); PAEC (Pakistan); MES and NSC (Poland); FCT (Portugal); MESTD (Serbia); MCIN/AEI and PCTI (Spain); MoSTR (Sri Lanka); Swiss Funding Agencies (Switzerland); MST (Taipei); MHESI and NSTDA (Thailand); TUBITAK and TENMAK (Turkey); NASU (Ukraine); STFC (United Kingdom); DOE and NSF (USA).

Individuals have received support from the Marie-Curie programme and the European Research Council and Horizon 2020 Grant, contract Nos. 675440, 724704, 752730, 758316, 765710, 824093, 884104, and COST Action CA16108 (European Union); the Leventis Foundation; the Alfred P. Sloan Foundation; the Alexander von Humboldt Foundation; the Belgian Federal Science Policy Office; the Fonds pour la Formation à la Recherche dans l'Industrie et dans l'Agriculture (FRIA-Belgium); the Agentschap voor Innovatie door Wetenschap en Technologie (IWT-Belgium); the F.R.S.-FNRS and FWO (Belgium) under the "Excellence of Science – EOS" – be.h project n. 30820817; the Beijing Municipal Science & Technology Commission, No. Z191100007219010; The Ministry of Education, Youth and Sports (MEYS) of the Czech Republic; the Hellenic Foundation for Research and Innovation (HFRI), Project Number 2288 (Greece); the Deutsche Forschungsgemeinschaft (DFG), under Germany's Excellence Strategy – EXC 2121 "Quantum Universe" – 390833306, and under project number 400140256 - GRK2497; the Hungarian Academy of Sciences, the New National Excellence Program - ÚNKP, the NKFIH research grants K 124845, K 124850, K 128713, K 128786, K 129058, K 131991, K 133046, K 138136, K 143460, K 143477, 2020-2.2.1-ED-2021-00181, and TKP2021-NKTA-64 (Hungary); the Council of Science and Industrial Research, India; the Latvian Council of Science; the Ministry of Education and Science, project no. 2022/WK/14, and the National Science Center, contracts Opus 2021/41/B/ST2/01369 and 2021/43/B/ST2/01552 (Poland); the Fundação para a Ciência e a Tecnologia, grant CEECIND/01334/2018 (Portugal); the National Priorities Research Program by Qatar National Research Fund; MCIN/AEI/10.13039/501100011033, ERDF "a way of making Europe", and the Programa Estatal de Fomento de la Investigación Científica y Técnica de Excelencia María de Maeztu, grant MDM-2017-0765 and Programa Severo Ochoa del Principado de Asturias (Spain); the Chulalongkorn Academic into Its 2nd Century Project Advancement Project, and the National Science, Research and Innovation Fund via the Program Management Unit for Human Resources & Institutional Development, Research and Innovation, grant B05F650021 (Thailand); the Kavli Foundation; the Nvidia Corporation; the SuperMicro Corporation; the Welch Foundation, contract C-1845; and the Weston Havens Foundation (USA).

References

[1] N. Cabibbo, Unitary symmetry and leptonic decays, Phys. Rev. Lett. 10 (1963) 531, https://doi.org/10.1103/PhysRevLett.10.531.

[2] M. Kobayashi, T. Maskawa, CP-violation in the renormalizable theory of weak interaction, Prog. Theor. Phys. 49 (1973) 652, https://doi.org/10.1143/PTP.49.652.

[3] M. Beneke, C. Bobeth, R. Szafron, Power-enhanced leading-logarithmic QED corrections to $B_q \to \mu^+\mu^-$, J. High Energy Phys. 10 (2019) 232, https://doi.org/10.1007/JHEP10(2019)232, arXiv:1908.07011.

[4] C. Bobeth, A.J. Buras, Searching for new physics with $\overline{\mathcal{B}}(B_{s,d} \to \mu\overline{\mu})/\Delta M_{s,d}$, Acta Phys. Pol. B 52 (2021) 1189, https://doi.org/10.5506/APhysPolB.52.1189, arXiv:2104.09521.

[5] CMS LHCb Collaborations, Observation of the rare $B_s^0 \to \mu^+\mu^-$ decay from the combined analysis of CMS and LHCb data, Nature 522 (2015) 68, https://doi.org/10.1038/nature14474, arXiv:1411.4413.

[6] ATLAS Collaboration, Study of the rare decays of B_s^0 and B^0 mesons into muon pairs using data collected during 2015 and 2016 with the ATLAS detector, J. High Energy Phys. 04 (2019) 098, https://doi.org/10.1007/JHEP04(2019)098, arXiv:1812.03017.

[7] CMS Collaboration, Measurement of properties of $B_s^0 \to \mu^+\mu^-$ decays and search for $B^0 \to \mu^+\mu^-$ with the CMS experiment, J. High Energy Phys. 04 (2020) 188, https://doi.org/10.1007/JHEP04(2020)188, arXiv:1910.12127.

[8] LHCb Collaboration, Measurement of the $B_s^0 \to \mu^+\mu^-$ branching fraction and effective lifetime and search for $B^0 \to \mu^+\mu^-$ decays, Phys. Rev. Lett. 118 (2017) 191801, https://doi.org/10.1103/PhysRevLett.118.191801, arXiv:1703.05747.

[9] LHCb Collaboration, Measurement of the $B_s^0 \to \mu^+\mu^-$ decay properties and search for the $B^0 \to \mu^+\mu^-$ and $B_s^0 \to \mu^+\mu^-\gamma$ decays, Phys. Rev. D 105 (2022) 012010, https://doi.org/10.1103/PhysRevD.105.012010, arXiv:2108.09283.

[10] LHCb Collaboration, Analysis of neutral B-meson decays into two muons, Phys. Rev. Lett. 128 (2022) 041801, https://doi.org/10.1103/PhysRevLett.128.041801, arXiv:2108.09284.

[11] ATLAS Collaboration, CMS Collaboration, LHCb Collaboration, Combination of the ATLAS, CMS and LHCb results on the $B_s^0 \to \mu^+\mu^-$ decays, Physics Analysis Summary CMS-PAS-BPH-20-003, LHCb-CONF-2020-002, ATLAS-CONF-2020-049, https://cds.cern.ch/record/2727216, 2020.

[12] LHCb Collaboration, Differential branching fractions and isospin asymmetries of $B \to K^*\mu^+\mu^-$ decays, J. High Energy Phys. 06 (2014) 133, https://doi.org/10.1007/JHEP06(2014)133, arXiv:1403.8044.

[13] LHCb Collaboration, Angular analysis of the rare decay $B_s^0 \to \phi\mu^+\mu^-$, J. High Energy Phys. 11 (2021) 043, https://doi.org/10.1007/JHEP11(2021)043, arXiv:2107.13428.

[14] LHCb Collaboration, Measurements of the S-wave fraction in $B^0 \to K^+\pi^-\mu^+\mu^-$ decays and the $B^0 \to K^*(892)^0\mu^+\mu^-$ differential branching fraction, J. High Energy Phys. 11 (2016) 047, https://doi.org/10.1007/JHEP11(2016)047, arXiv:1606.04731, Erratum: https://doi.org/10.1007/JHEP04(2017)142.

[15] LHCb Collaboration, Branching fraction measurements of the rare $B_s^0 \to \phi\mu^+\mu^-$ and $B_s^0 \to f_2'(1525)\mu^+\mu^-$ decays, Phys. Rev. Lett. 127 (2021) 151801, https://doi.org/10.1103/PhysRevLett.127.151801, arXiv:2105.14007.

[16] LHCb Collaboration, Measurement of CP-averaged observables in the $B^0 \to K^{*0}\mu^+\mu^-$ decay, Phys. Rev. Lett. 125 (2020) 011802, https://doi.org/10.1103/PhysRevLett.125.011802, arXiv:2003.04831.

[17] LHCb Collaboration, Angular analysis of the $B^+ \to K^{*+}\mu^+\mu^-$ decay, Phys. Rev. Lett. 126 (2021) 161802, https://doi.org/10.1103/PhysRevLett.126.161802, arXiv:2012.13241.

[18] LHCb Collaboration, Test of lepton universality with $B^0 \to K^{*0}\ell^+\ell^-$ decays, J. High Energy Phys. 08 (2017) 055, https://doi.org/10.1007/JHEP08(2017)055, arXiv:1705.05802.

[19] LHCb Collaboration, Test of lepton universality in beauty-quark decays, Nat. Phys. 18 (2022) 277, https://doi.org/10.1038/s41567-021-01478-8, arXiv:2103.11769.

[20] A. Abdesselam, et al., Belle, Test of lepton-flavor universality in $B \to K^*\ell^+\ell^-$ decays at Belle, Phys. Rev. Lett. 126 (2021) 161801, https://doi.org/10.1103/PhysRevLett.126.161801, arXiv:1904.02440.

[21] S. Choudhury, et al., Belle, Test of lepton flavor universality and search for lepton flavor violation in $B \to K\ell\ell$ decays, J. High Energy Phys. 03 (2021) 105, https://doi.org/10.1007/JHEP03(2021)105, arXiv:1908.01848.

[22] LHCb Collaboration, Tests of lepton universality using $B^0 \to K^0_S\ell^+\ell^-$ and $B^+ \to K^{*+}\ell^+\ell^-$ decays, Phys. Rev. Lett. 128 (2022) 191802, https://doi.org/10.1103/PhysRevLett.128.191802, arXiv:2110.09501.

[23] CMS Collaboration, Angular analysis of the decay $B^0 \to K^{*0}\mu^+\mu^-$ from pp collisions at $\sqrt{s} = 8$ TeV, Phys. Lett. B 753 (2016) 424, https://doi.org/10.1016/j.physletb.2015.12.020, arXiv:1507.08126.

[24] CMS Collaboration, Measurement of angular parameters from the decay $B^0 \to K^{*0}\mu^+\mu^-$ in proton-proton collisions at $\sqrt{s} = 8$ TeV, Phys. Lett. B 781 (2018) 517, https://doi.org/10.1016/j.physletb.2018.04.030, arXiv:1710.02846.

[25] LHCb Collaboration, Test of lepton universality in $b \to s\ell^+\ell^-$ decays, arXiv:2212.09152, 2022.

[26] LHCb Collaboration, Measurement of lepton universality parameters in $B^+ \to K^+\ell^+\ell^-$ and $B^0 \to K^{*0}\ell^+\ell^-$ decays, arXiv:2212.09153, 2022.

[27] Flavour Lattice Averaging Group (FLAG), FLAG review 2021, Eur. Phys. J. C 82 (2022) 869, https://doi.org/10.1140/epjc/s10052-022-10536-1, arXiv:2111.09849.

[28] Y. Amhis, et al., HFLAV, Averages of b-hadron, c-hadron, and τ-lepton properties as of 2021, arXiv:2206.07501, 2022.

[29] Particle Data Group, R.L. Workman, et al., Review of particle physics, PTEP 2022 (2022) 083C01, https://doi.org/10.1093/ptep/ptac097.

[30] HEPData record for this analysis, https://doi.org/10.17182/hepdata.135675, 2022.

[31] CMS Collaboration, The CMS experiment at the CERN LHC, J. Instrum. 3 (2008) S08004, https://doi.org/10.1088/1748-0221/3/08/S08004.

[32] CMS Collaboration, Description and performance of track and primary-vertex reconstruction with the CMS tracker, J. Instrum. 9 (2014) P10009, https://doi.org/10.1088/1748-0221/9/10/P10009, arXiv:1405.6569.

[33] CMS Tracker Group, The CMS Phase-1 pixel detector upgrade, J. Instrum. 16 (2021) P02027, https://doi.org/10.1088/1748-0221/16/02/P02027, arXiv:2012.14304.

[34] CMS Collaboration, Track impact parameter resolution for the full pseudorapidity coverage in the 2017 dataset with the CMS Phase-1 Pixel detector, CMS Detector Performance Report CMS-DP-2020-049, 2020, https://cds.cern.ch/record/2743740.

[35] CMS Collaboration, Performance of the CMS muon detector and muon reconstruction with proton-proton collisions at $\sqrt{s} = 13$ TeV, J. Instrum. 13 (2018) P06015, https://doi.org/10.1088/1748-0221/13/06/P06015, arXiv:1804.04528.

[36] CMS Collaboration, Performance of the CMS Level-1 trigger in proton-proton collisions at $\sqrt{s} = 13$ TeV, J. Instrum. 15 (2020) P10017, https://doi.org/10.1088/1748-0221/15/10/P10017, arXiv:2006.10165.

[37] CMS Collaboration, The CMS trigger system, J. Instrum. 12 (2017) P01020, https://doi.org/10.1088/1748-0221/12/01/P01020, arXiv:1609.02366.

[38] CMS Collaboration, Precision luminosity measurement in proton-proton collisions at $\sqrt{s} = 13$ TeV in 2015 and 2016 at CMS, Eur. Phys. J. C 81 (2021) 800, https://doi.org/10.1140/epjc/s10052-021-09538-2, arXiv:2104.01927.

[39] CMS Collaboration, CMS luminosity measurements for the 2017 data-taking period at $\sqrt{s} = 13$ TeV, CMS Physics Analysis Summary CMS-PAS-LUM-17-004, https://cds.cern.ch/record/2621960, 2018.

[40] CMS Collaboration, CMS luminosity measurements for the 2018 data-taking period at $\sqrt{s} = 13$ TeV, CMS Physics Analysis Summary CMS-PAS-LUM-18-001, https://cds.cern.ch/record/2676164, 2018.

[41] T. Sjöstrand, S. Ask, J.R. Christiansen, R. Corke, N. Desai, P. Ilten, S. Mrenna, S. Prestel, C.O. Rasmussen, P.Z. Skands, An introduction to PYTHIA 8.2, Comput. Phys. Commun. 191 (2015) 159, https://doi.org/10.1016/j.cpc.2015.01.024, arXiv:1410.3012.

[42] CMS Collaboration, Extraction and validation of a new set of CMS PYTHIA8 tunes from underlying-event measurements, Eur. Phys. J. C 80 (2020) 4, https://doi.org/10.1140/epjc/s10052-019-7499-4, arXiv:1903.12179.

[43] S. Agostinelli, et al., GEANT4, Geant4—a simulation toolkit, Nucl. Instrum. Methods A 506 (2003) 250, https://doi.org/10.1016/S0168-9002(03)01368-8.

[44] D.J. Lange, The EvtGen particle decay simulation package, Nucl. Instrum. Methods A 462 (2001) 152, https://doi.org/10.1016/S0168-9002(01)00089-4.

[45] N. Davidson, T. Przedzinski, Z. Was, PHOTOS interface in C++: technical and physics documentation, Comput. Phys. Commun. 199 (2016) 86, https://doi.org/10.1016/j.cpc.2015.09.013, arXiv:1011.0937.

[46] K. Prokofiev, T. Speer, A kinematic and a decay chain reconstruction library, in: Proc. Int. Conf. on Comput. in High-Energy and Nuc. Physics (CHEP '04), 2004, p. 411, https://doi.org/10.5170/CERN-2005-002.

[47] T. Chen, C. Guestrin, XGBoost: a scalable tree boosting system, in: Proc. 22nd ACM SIGKDD Int. Conf. on Knowledge Discovery and Data Mining, KDD '16, ACM, New York, NY, USA, 2016, p. 785, https://doi.org/10.1145/2939672.2939785.

[48] M. Pivk, F.R. Le Diberder, ${}_s\mathcal{P}lot$: a statistical tool to unfold data distributions, Nucl. Instrum. Methods A 555 (2005) 356, https://doi.org/10.1016/j.nima.2005.08.106, arXiv:physics/0402083.

[49] M.J. Oreglia, A study of the reactions $\psi' \to \gamma\gamma\psi$, Ph.D. thesis, Stanford University, 1980, http://www.slac.stanford.edu/pubs/cgi-wrap/getdoc/slac-r-236.pdf, SLAC Report SLAC-R-236.

[50] CMS Collaboration, Tracking performances for charged pions with Run2 legacy data, CMS Detector Performance Report CMS-DP-2022-012, 2022, https://cds.cern.ch/record/2810814.

[51] LHCb Collaboration, Precise measurement of the f_s/f_d ratio of fragmentation fractions and of B^0_s decay branching fractions, Phys. Rev. D 104 (2021) 032005, https://doi.org/10.1103/PhysRevD.104.032005, arXiv:2103.06810.

[52] CMS Collaboration, Measurement of the dependence of the hadron production fraction ratio f_s/f_u on B meson kinematic variables in proton-proton collisions at $\sqrt{s}$ = 13 TeV, submitted to Phys. Rev. Lett., arXiv:2212.02309, 2022.

[53] W. Altmannshofer, et al., Belle-II, The Belle II physics book, PTEP 2019, PTEP 2019 (2020) 123C01, https://doi.org/10.1093/ptep/ptz106, arXiv:1808.10567, 2019, Erratum: PTEP 2020 (2020) 029201.

[54] T. Junk, Confidence level computation for combining searches with small statistics, Nucl. Instrum. Methods A 434 (1999) 435, https://doi.org/10.1016/S0168-9002(99)00498-2, arXiv:hep-ex/9902006.

[55] A.L. Read, Presentation of search results: the CL_s technique, J. Phys. G 28 (2002) 2693, https://doi.org/10.1088/0954-3899/28/10/313.

[56] W. Altmannshofer, P. Stangl, New physics in rare B decays after Moriond 2021, Eur. Phys. J. C 81 (2021) 952, https://doi.org/10.1140/epjc/s10052-021-09725-1, arXiv:2103.13370.

The CMS Collaboration

A. Tumasyan [1]

Yerevan Physics Institute, Yerevan, Armenia

W. Adam, J.W. Andrejkovic, T. Bergauer, S. Chatterjee, K. Damanakis, M. Dragicevic, A. Escalante Del Valle, P.S. Hussain, M. Jeitler [2], N. Krammer, L. Lechner, D. Liko, I. Mikulec, P. Paulitsch, F.M. Pitters, J. Schieck [2], R. Schöfbeck, D. Schwarz, M. Sonawane, S. Templ, W. Waltenberger, C.-E. Wulz [2]

Institut für Hochenergiephysik, Vienna, Austria

M.R. Darwish [3], T. Janssen, T. Kello [4], H. Rejeb Sfar, P. Van Mechelen

Universiteit Antwerpen, Antwerpen, Belgium

E.S. Bols, J. D'Hondt, A. De Moor, M. Delcourt, H. El Faham, S. Lowette, S. Moortgat, A. Morton, D. Müller, A.R. Sahasransu, S. Tavernier, W. Van Doninck, D. Vannerom

Vrije Universiteit Brussel, Brussel, Belgium

B. Clerbaux, G. De Lentdecker, L. Favart, D. Hohov, J. Jaramillo, K. Lee, M. Mahdavikhorrami, I. Makarenko, A. Malara, S. Paredes, L. Pétré, N. Postiau, L. Thomas, M. Vanden Bemden, C. Vander Velde, P. Vanlaer

Université Libre de Bruxelles, Bruxelles, Belgium

D. Dobur, J. Knolle, L. Lambrecht, G. Mestdach, C. Rendón, A. Samalan, K. Skovpen, M. Tytgat, N. Van Den Bossche, B. Vermassen, L. Wezenbeek

Ghent University, Ghent, Belgium

A. Benecke, G. Bruno, F. Bury, C. Caputo, P. David, C. Delaere, I.S. Donertas, A. Giammanco, K. Jaffel, Sa. Jain, V. Lemaitre, K. Mondal, A. Taliercio, T.T. Tran, P. Vischia, S. Wertz

Université Catholique de Louvain, Louvain-la-Neuve, Belgium

G.A. Alves, E. Coelho, C. Hensel, A. Moraes, P. Rebello Teles

Centro Brasileiro de Pesquisas Fisicas, Rio de Janeiro, Brazil

W.L. Aldá Júnior, M. Alves Gallo Pereira, M. Barroso Ferreira Filho, H. Brandao Malbouisson, W. Carvalho, J. Chinellato [5], E.M. Da Costa, G.G. Da Silveira [6], D. De Jesus Damiao, V. Dos Santos Sousa, S. Fonseca De Souza, J. Martins [7], C. Mora Herrera, K. Mota Amarilo, L. Mundim, H. Nogima, A. Santoro, S.M. Silva Do Amaral, A. Sznajder, M. Thiel, A. Vilela Pereira

Universidade do Estado do Rio de Janeiro, Rio de Janeiro, Brazil

C.A. Bernardes [6], L. Calligaris, T.R. Fernandez Perez Tomei, E.M. Gregores, P.G. Mercadante, S.F. Novaes, Sandra S. Padula

Universidade Estadual Paulista, Universidade Federal do ABC, São Paulo, Brazil

A. Aleksandrov, G. Antchev, R. Hadjiiska, P. Iaydjiev, M. Misheva, M. Rodozov, M. Shopova, G. Sultanov

Institute for Nuclear Research and Nuclear Energy, Bulgarian Academy of Sciences, Sofia, Bulgaria

A. Dimitrov, T. Ivanov, L. Litov, B. Pavlov, P. Petkov, A. Petrov, E. Shumka

University of Sofia, Sofia, Bulgaria

S. Thakur

Instituto De Alta Investigación - Universidad de Tarapacá, Casilla 7 D, Arica, Chile

T. Cheng, T. Javaid [8], M. Mittal, L. Yuan

Beihang University, Beijing, China

M. Ahmad, G. Bauer [9], Z. Hu, S. Lezki, K. Yi [9,10]

Department of Physics, Tsinghua University, Beijing, China

G.M. Chen [8], H.S. Chen [8], M. Chen [8], F. Iemmi, C.H. Jiang, A. Kapoor, H. Liao, Z.-A. Liu [11], V. Milosevic, F. Monti, R. Sharma, J. Tao, J. Thomas-Wilsker, J. Wang, H. Zhang, J. Zhao

Institute of High Energy Physics, Beijing, China

A. Agapitos, Y. An, Y. Ban, A. Levin, C. Li, Q. Li, X. Lyu, Y. Mao, S.J. Qian, X. Sun, D. Wang, J. Xiao, H. Yang

State Key Laboratory of Nuclear Physics and Technology, Peking University, Beijing, China

M. Lu, Z. You

Sun Yat-Sen University, Guangzhou, China

N. Lu

University of Science and Technology of China, Hefei, China

X. Gao [4], D. Leggat, H. Okawa, Y. Zhang

Institute of Modern Physics and Key Laboratory of Nuclear Physics and Ion-beam Application (MOE) - Fudan University, Shanghai, China

Z. Lin, C. Lu, M. Xiao

Zhejiang University, Hangzhou, Zhejiang, China

C. Avila, D.A. Barbosa Trujillo, A. Cabrera, C. Florez, J. Fraga

Universidad de Los Andes, Bogota, Colombia

J. Mejia Guisao, F. Ramirez, M. Rodriguez, J.D. Ruiz Alvarez

Universidad de Antioquia, Medellin, Colombia

D. Giljanovic, N. Godinovic, D. Lelas, I. Puljak

University of Split, Faculty of Electrical Engineering, Mechanical Engineering and Naval Architecture, Split, Croatia

Z. Antunovic, M. Kovac, T. Sculac

University of Split, Faculty of Science, Split, Croatia

V. Brigljevic, B.K. Chitroda, D. Ferencek, S. Mishra, M. Roguljic, A. Starodumov [12], T. Susa

Institute Rudjer Boskovic, Zagreb, Croatia

A. Attikis, K. Christoforou, M. Kolosova, S. Konstantinou, J. Mousa, C. Nicolaou, F. Ptochos, P.A. Razis, H. Rykaczewski, H. Saka, A. Stepennov

University of Cyprus, Nicosia, Cyprus

M. Finger, M. Finger Jr., A. Kveton

Charles University, Prague, Czech Republic

E. Ayala

Escuela Politecnica Nacional, Quito, Ecuador

E. Carrera Jarrin

Universidad San Francisco de Quito, Quito, Ecuador

S. Elgammal [13], A. Ellithi Kamel [14]

Academy of Scientific Research and Technology of the Arab Republic of Egypt, Egyptian Network of High Energy Physics, Cairo, Egypt

A. Lotfy, M.A. Mahmoud

Center for High Energy Physics (CHEP-FU), Fayoum University, El-Fayoum, Egypt

S. Bhowmik, R.K. Dewanjee, K. Ehataht, M. Kadastik, T. Lange, S. Nandan, C. Nielsen, J. Pata, M. Raidal, L. Tani, C. Veelken

National Institute of Chemical Physics and Biophysics, Tallinn, Estonia

P. Eerola, H. Kirschenmann, K. Osterberg, M. Voutilainen

Department of Physics, University of Helsinki, Helsinki, Finland

S. Bharthuar, E. Brücken, F. Garcia, J. Havukainen, M.S. Kim, R. Kinnunen, T. Lampén, K. Lassila-Perini, S. Lehti, T. Lindén, M. Lotti, L. Martikainen, M. Myllymäki, J. Ott, M.m. Rantanen, H. Siikonen, E. Tuominen, J. Tuominiemi

Helsinki Institute of Physics, Helsinki, Finland

P. Luukka, H. Petrow, T. Tuuva

Lappeenranta-Lahti University of Technology, Lappeenranta, Finland

C. Amendola, M. Besancon, F. Couderc, M. Dejardin, D. Denegri, J.L. Faure, F. Ferri, S. Ganjour, P. Gras, G. Hamel de Monchenault, V. Lohezic, J. Malcles, J. Rander, A. Rosowsky, M.Ö. Sahin, A. Savoy-Navarro [15], P. Simkina, M. Titov

IRFU, CEA, Université Paris-Saclay, Gif-sur-Yvette, France

C. Baldenegro Barrera, F. Beaudette, A. Buchot Perraguin, A. Cappati, C. Charlot, F. Damas, O. Davignon, B. Diab, G. Falmagne, B.A. Fontana Santos Alves, S. Ghosh, R. Granier de Cassagnac, A. Hakimi, B. Harikrishnan, G. Liu, J. Motta, M. Nguyen, C. Ochando, L. Portales, R. Salerno, U. Sarkar, J.B. Sauvan, Y. Sirois, A. Tarabini, E. Vernazza, A. Zabi, A. Zghiche

Laboratoire Leprince-Ringuet, CNRS/IN2P3, Ecole Polytechnique, Institut Polytechnique de Paris, Palaiseau, France

J.-L. Agram [16], J. Andrea, D. Apparu, D. Bloch, G. Bourgatte, J.-M. Brom, E.C. Chabert, C. Collard, D. Darej, U. Goerlach, C. Grimault, A.-C. Le Bihan, P. Van Hove

Université de Strasbourg, CNRS, IPHC UMR 7178, Strasbourg, France

S. Beauceron, B. Blancon, G. Boudoul, A. Carle, N. Chanon, J. Choi, D. Contardo, P. Depasse, C. Dozen [17], H. El Mamouni, J. Fay, S. Gascon, M. Gouzevitch, G. Grenier, B. Ille, I.B. Laktineh, M. Lethuillier, L. Mirabito, S. Perries, L. Torterotot, M. Vander Donckt, P. Verdier, S. Viret

Institut de Physique des 2 Infinis de Lyon (IP2I), Villeurbanne, France

I. Bagaturia [18], I. Lomidze, Z. Tsamalaidze [12]

Georgian Technical University, Tbilisi, Georgia

V. Botta, L. Feld, K. Klein, M. Lipinski, D. Meuser, A. Pauls, N. Röwert, M. Teroerde

RWTH Aachen University, I. Physikalisches Institut, Aachen, Germany

S. Diekmann, A. Dodonova, N. Eich, D. Eliseev, M. Erdmann, P. Fackeldey, D. Fasanella, B. Fischer, T. Hebbeker, K. Hoepfner, F. Ivone, M.y. Lee, L. Mastrolorenzo, M. Merschmeyer, A. Meyer, S. Mondal, S. Mukherjee, D. Noll, A. Novak, F. Nowotny, A. Pozdnyakov, Y. Rath, W. Redjeb, H. Reithler, A. Schmidt, S.C. Schuler, A. Sharma, A. Stein, F. Torres Da Silva De Araujo [19], L. Vigilante, S. Wiedenbeck, S. Zaleski

RWTH Aachen University, III. Physikalisches Institut A, Aachen, Germany

C. Dziwok, G. Flügge, W. Haj Ahmad [20], O. Hlushchenko, T. Kress, A. Nowack, O. Pooth, A. Stahl, T. Ziemons, A. Zotz

RWTH Aachen University, III. Physikalisches Institut B, Aachen, Germany

H. Aarup Petersen, M. Aldaya Martin, P. Asmuss, S. Baxter, M. Bayatmakou, O. Behnke, A. Bermúdez Martínez, S. Bhattacharya, A.A. Bin Anuar, F. Blekman [21], K. Borras [22], D. Brunner, A. Campbell, A. Cardini, C. Cheng, F. Colombina, S. Consuegra Rodríguez, G. Correia Silva, M. De Silva, L. Didukh, G. Eckerlin, D. Eckstein, L.I. Estevez Banos, O. Filatov, E. Gallo [21], A. Geiser, A. Giraldi, G. Greau, A. Grohsjean, V. Guglielmi, M. Guthoff, A. Jafari [23], N.Z. Jomhari, B. Kaech, M. Kasemann, H. Kaveh, C. Kleinwort, R. Kogler, M. Komm, D. Krücker, W. Lange, D. Leyva Pernia, K. Lipka [24], W. Lohmann [25], R. Mankel, I.-A. Melzer-Pellmann, M. Mendizabal Morentin, J. Metwally, A.B. Meyer,

G. Milella, M. Mormile, A. Mussgiller, A. Nürnberg, Y. Otarid, D. Pérez Adán, A. Raspereza, B. Ribeiro Lopes, J. Rübenach, A. Saggio, A. Saibel, M. Savitskyi, M. Scham [26,22], V. Scheurer, S. Schnake [22], P. Schütze, C. Schwanenberger [21], M. Shchedrolosiev, R.E. Sosa Ricardo, D. Stafford, N. Tonon [†], M. Van De Klundert, F. Vazzoler, A. Ventura Barroso, R. Walsh, D. Walter, Q. Wang, Y. Wen, K. Wichmann, L. Wiens [22], C. Wissing, S. Wuchterl, Y. Yang, A. Zimermmane Castro Santos

Deutsches Elektronen-Synchrotron, Hamburg, Germany

A. Albrecht, S. Albrecht, M. Antonello, S. Bein, L. Benato, M. Bonanomi, P. Connor, K. De Leo, M. Eich, K. El Morabit, F. Feindt, A. Fröhlich, C. Garbers, E. Garutti, M. Hajheidari, J. Haller, A. Hinzmann, H.R. Jabusch, G. Kasieczka, P. Keicher, R. Klanner, W. Korcari, T. Kramer, V. Kutzner, F. Labe, J. Lange, A. Lobanov, C. Matthies, A. Mehta, L. Moureaux, M. Mrowietz, A. Nigamova, Y. Nissan, A. Paasch, K.J. Pena Rodriguez, T. Quadfasel, M. Rieger, O. Rieger, D. Savoiu, J. Schindler, P. Schleper, M. Schröder, J. Schwandt, M. Sommerhalder, H. Stadie, G. Steinbrück, A. Tews, M. Wolf

University of Hamburg, Hamburg, Germany

S. Brommer, M. Burkart, E. Butz, T. Chwalek, A. Dierlamm, A. Droll, N. Faltermann, M. Giffels, J.O. Gosewisch, A. Gottmann, F. Hartmann [27], M. Horzela, U. Husemann, M. Klute, R. Koppenhöfer, M. Link, A. Lintuluoto, S. Maier, S. Mitra, Th. Müller, M. Neukum, M. Oh, G. Quast, K. Rabbertz, J. Rauser, I. Shvetsov, H.J. Simonis, N. Trevisani, R. Ulrich, J. van der Linden, R.F. Von Cube, M. Wassmer, S. Wieland, R. Wolf, S. Wozniewski, S. Wunsch, X. Zuo

Karlsruher Institut fuer Technologie, Karlsruhe, Germany

G. Anagnostou, P. Assiouras, G. Daskalakis, A. Kyriakis, A. Stakia

Institute of Nuclear and Particle Physics (INPP), NCSR Demokritos, Aghia Paraskevi, Greece

M. Diamantopoulou, D. Karasavvas, P. Kontaxakis, A. Manousakis-Katsikakis, A. Panagiotou, I. Papavergou, N. Saoulidou, K. Theofilatos, E. Tziaferi, K. Vellidis, I. Zisopoulos

National and Kapodistrian University of Athens, Athens, Greece

G. Bakas, T. Chatzistavrou, K. Kousouris, I. Papakrivopoulos, G. Tsipolitis, A. Zacharopoulou

National Technical University of Athens, Athens, Greece

K. Adamidis, I. Bestintzanos, I. Evangelou, C. Foudas, P. Gianneios, C. Kamtsikis, P. Katsoulis, P. Kokkas, P.G. Kosmoglou Kioseoglou, N. Manthos, I. Papadopoulos, J. Strologas

University of Ioánnina, Ioánnina, Greece

M. Csanád, K. Farkas, M.M.A. Gadallah [28], S. Lökös [29], P. Major, K. Mandal, G. Pásztor, A.J. Rádl [30], O. Surányi, G.I. Veres

MTA-ELTE Lendület CMS Particle and Nuclear Physics Group, Eötvös Loránd University, Budapest, Hungary

M. Bartók [31], G. Bencze, C. Hajdu, D. Horvath [32,33], F. Sikler, V. Veszpremi

Wigner Research Centre for Physics, Budapest, Hungary

N. Beni, S. Czellar, J. Karancsi [31], J. Molnar, Z. Szillasi, D. Teyssier

Institute of Nuclear Research ATOMKI, Debrecen, Hungary

P. Raics, B. Ujvari [34]

Institute of Physics, University of Debrecen, Debrecen, Hungary

T. Csorgo [30], F. Nemes [30], T. Novak

Karoly Robert Campus, MATE Institute of Technology, Gyongyos, Hungary

J. Babbar, S. Bansal, S.B. Beri, V. Bhatnagar, G. Chaudhary, S. Chauhan, N. Dhingra [35], R. Gupta, A. Kaur, A. Kaur, H. Kaur, M. Kaur, S. Kumar, P. Kumari, M. Meena, K. Sandeep, T. Sheokand, J.B. Singh [36], A. Singla, A.K. Virdi

Panjab University, Chandigarh, India

A. Ahmed, A. Bhardwaj, A. Chhetri, B.C. Choudhary, A. Kumar, M. Naimuddin, K. Ranjan, S. Saumya

University of Delhi, Delhi, India

S. Baradia, S. Barman [37], S. Bhattacharya, D. Bhowmik, S. Dutta, S. Dutta, B. Gomber [38], M. Maity [37], P. Palit, G. Saha, B. Sahu, S. Sarkar

Saha Institute of Nuclear Physics, HBNI, Kolkata, India

P.K. Behera, S.C. Behera, S. Chatterjee, P. Kalbhor, J.R. Komaragiri [39], D. Kumar [39], A. Muhammad, L. Panwar [39], R. Pradhan, P.R. Pujahari, N.R. Saha, A. Sharma, A.K. Sikdar, S. Verma

Indian Institute of Technology Madras, Madras, India

K. Naskar [40]

Bhabha Atomic Research Centre, Mumbai, India

T. Aziz, I. Das, S. Dugad, M. Kumar, G.B. Mohanty, P. Suryadevara

Tata Institute of Fundamental Research-A, Mumbai, India

S. Banerjee, R. Chudasama, M. Guchait, S. Karmakar, S. Kumar, G. Majumder, K. Mazumdar, S. Mukherjee, A. Thachayath

Tata Institute of Fundamental Research-B, Mumbai, India

S. Bahinipati [41], A.K. Das, C. Kar, P. Mal, T. Mishra, V.K. Muraleedharan Nair Bindhu [42], A. Nayak [42], P. Saha, S.K. Swain, D. Vats [42]

National Institute of Science Education and Research, An OCC of Homi Bhabha National Institute, Bhubaneswar, Odisha, India

A. Alpana, S. Dube, B. Kansal, A. Laha, S. Pandey, A. Rastogi, S. Sharma

Indian Institute of Science Education and Research (IISER), Pune, India

H. Bakhshiansohi [43], E. Khazaie, M. Zeinali [44]

Isfahan University of Technology, Isfahan, Iran

S. Chenarani [45], S.M. Etesami, M. Khakzad, M. Mohammadi Najafabadi

Institute for Research in Fundamental Sciences (IPM), Tehran, Iran

M. Grunewald

University College Dublin, Dublin, Ireland

M. Abbrescia [a,b], R. Aly [a,c,46], C. Aruta [a,b], A. Colaleo [a], D. Creanza [a,c], N. De Filippis [a,c], M. De Palma [a,b], A. Di Florio [a,b], W. Elmetenawee [a,b], F. Errico [a,b], L. Fiore [a], G. Iaselli [a,c], G. Maggi [a,c], M. Maggi [a], I. Margjeka [a,b], V. Mastrapasqua [a,b], S. My [a,b], S. Nuzzo [a,b], A. Pellecchia [a,b], A. Pompili [a,b], G. Pugliese [a,c], R. Radogna [a], D. Ramos [a], A. Ranieri [a], G. Selvaggi [a,b], L. Silvestris [a], F.M. Simone [a,b], Ü. Sözbilir [a], A. Stamerra [a], R. Venditti [a], P. Verwilligen [a]

[a] *INFN Sezione di Bari, Bari, Italy*
[b] *Università di Bari, Bari, Italy*
[c] *Politecnico di Bari, Bari, Italy*

G. Abbiendi [a], C. Battilana [a,b], D. Bonacorsi [a,b], L. Borgonovi [a], L. Brigliadori [a], R. Campanini [a,b], P. Capiluppi [a,b], A. Castro [a,b], F.R. Cavallo [a], M. Cuffiani [a,b], G.M. Dallavalle [a], T. Diotalevi [a,b], F. Fabbri [a],

A. Fanfani [a,b], P. Giacomelli [a], L. Giommi [a,b], C. Grandi [a], L. Guiducci [a,b], S. Lo Meo [a,47], L. Lunerti [a,b], S. Marcellini [a], G. Masetti [a], F.L. Navarria [a,b], A. Perrotta [a], F. Primavera [a,b], A.M. Rossi [a,b], T. Rovelli [a,b], G.P. Siroli [a,b]

[a] INFN Sezione di Bologna, Bologna, Italy
[b] Università di Bologna, Bologna, Italy

S. Costa [a,b,48], A. Di Mattia [a], R. Potenza [a,b], A. Tricomi [a,b,48], C. Tuve [a,b]

[a] INFN Sezione di Catania, Catania, Italy
[b] Università di Catania, Catania, Italy

G. Barbagli [a], G. Bardelli [a,b], B. Camaiani [a,b], A. Cassese [a], R. Ceccarelli [a,b], V. Ciulli [a,b], C. Civinini [a], R. D'Alessandro [a,b], E. Focardi [a,b], G. Latino [a,b], P. Lenzi [a,b], M. Lizzo [a,b], M. Meschini [a], S. Paoletti [a], R. Seidita [a,b], G. Sguazzoni [a], L. Viliani [a]

[a] INFN Sezione di Firenze, Firenze, Italy
[b] Università di Firenze, Firenze, Italy

L. Benussi, S. Bianco, S. Meola [49], D. Piccolo

INFN Laboratori Nazionali di Frascati, Frascati, Italy

M. Bozzo [a,b], P. Chatagnon [a], F. Ferro [a], E. Robutti [a], S. Tosi [a,b]

[a] INFN Sezione di Genova, Genova, Italy
[b] Università di Genova, Genova, Italy

A. Benaglia [a], G. Boldrini [a], F. Brivio [a,b], F. Cetorelli [a,b], F. De Guio [a,b], M.E. Dinardo [a,b], P. Dini [a], S. Gennai [a], A. Ghezzi [a,b], P. Govoni [a,b], L. Guzzi [a,b], M.T. Lucchini [a,b], M. Malberti [a], S. Malvezzi [a], A. Massironi [a], D. Menasce [a], L. Moroni [a], M. Paganoni [a,b], D. Pedrini [a], B.S. Pinolini [a], S. Ragazzi [a,b], N. Redaelli [a], T. Tabarelli de Fatis [a,b], D. Zuolo [a,b]

[a] INFN Sezione di Milano-Bicocca, Milano, Italy
[b] Università di Milano-Bicocca, Milano, Italy

S. Buontempo [a], F. Carnevali [a,b], N. Cavallo [a,c], A. De Iorio [a,b], F. Fabozzi [a,c], A.O.M. Iorio [a,b], L. Lista [a,b,50], P. Paolucci [a,27], B. Rossi [a], C. Sciacca [a,b]

[a] INFN Sezione di Napoli, Napoli, Italy
[b] Università di Napoli 'Federico II', Napoli, Italy
[c] Università della Basilicata, Potenza, Italy
[d] Università G. Marconi, Roma, Italy

N. Bacchetta [a,51], D. Bisello [a,b], P. Bortignon [a], A. Bragagnolo [a,b], R. Carlin [a,b], P. Checchia [a], T. Dorigo [a], F. Gasparini [a,b], U. Gasparini [a,b], G. Grosso [a], L. Layer [a,52], E. Lusiani [a], M. Margoni [a,b], A.T. Meneguzzo [a,b], M. Passaseo [a], J. Pazzini [a,b], P. Ronchese [a,b], R. Rossin [a,b], M. Sgaravatto [a], F. Simonetto [a,b], G. Strong [a], M. Tosi [a,b], H. Yarar [a,b], M. Zanetti [a,b], A. Zucchetta [a,b], G. Zumerle [a,b]

[a] INFN Sezione di Padova, Padova, Italy
[b] Università di Padova, Padova, Italy
[c] Università di Trento, Trento, Italy

S. Abu Zeid [a,53], C. Aimè [a,b], A. Braghieri [a], S. Calzaferri [a,b], D. Fiorina [a,b], P. Montagna [a,b], V. Re [a], C. Riccardi [a,b], P. Salvini [a], I. Vai [a], P. Vitulo [a,b]

[a] INFN Sezione di Pavia, Pavia, Italy
[b] Università di Pavia, Pavia, Italy

P. Asenov [a,54], G.M. Bilei [a], D. Ciangottini [a,b], L. Fanò [a,b], M. Magherini [a,b], G. Mantovani [a,b], V. Mariani [a,b], M. Menichelli [a], F. Moscatelli [a,54], A. Piccinelli [a,b], M. Presilla [a,b], A. Rossi [a,b], A. Santocchia [a,b], D. Spiga [a], T. Tedeschi [a,b]

[a] INFN Sezione di Perugia, Perugia, Italy
[b] Università di Perugia, Perugia, Italy

P. Azzurri [a], G. Bagliesi [a], V. Bertacchi [a,c], R. Bhattacharya [a], L. Bianchini [a,b], T. Boccali [a], E. Bossini [a,b], D. Bruschini [a,c], R. Castaldi [a], M.A. Ciocci [a,b], V. D'Amante [a,d], R. Dell'Orso [a], S. Donato [a], A. Giassi [a], F. Ligabue [a,c], D. Matos Figueiredo [a], A. Messineo [a,b], M. Musich [a,b], F. Palla [a], S. Parolia [a], G. Ramirez-Sanchez [a,c], A. Rizzi [a,b], G. Rolandi [a,c], S. Roy Chowdhury [a], T. Sarkar [a], A. Scribano [a], P. Spagnolo [a], R. Tenchini [a], G. Tonelli [a,b], N. Turini [a,d], A. Venturi [a], P.G. Verdini [a]

[a] *INFN Sezione di Pisa, Pisa, Italy*
[b] *Università di Pisa, Pisa, Italy*
[c] *Scuola Normale Superiore di Pisa, Pisa, Italy*
[d] *Università di Siena, Siena, Italy*

P. Barria [a], M. Campana [a,b], F. Cavallari [a], D. Del Re [a,b], E. Di Marco [a], M. Diemoz [a], E. Longo [a,b], P. Meridiani [a], G. Organtini [a,b], F. Pandolfi [a], R. Paramatti [a,b], C. Quaranta [a,b], S. Rahatlou [a,b], C. Rovelli [a], F. Santanastasio [a,b], L. Soffi [a], R. Tramontano [a,b]

[a] *INFN Sezione di Roma, Roma, Italy*
[b] *Sapienza Università di Roma, Roma, Italy*

N. Amapane [a,b], R. Arcidiacono [a,c], S. Argiro [a,b], M. Arneodo [a,c], N. Bartosik [a], R. Bellan [a,b], A. Bellora [a,b], C. Biino [a], N. Cartiglia [a], M. Costa [a,b], R. Covarelli [a,b], N. Demaria [a], M. Grippo [a,b], B. Kiani [a,b], F. Legger [a], C. Mariotti [a], S. Maselli [a], A. Mecca [a,b], E. Migliore [a,b], E. Monteil [a,b], M. Monteno [a], R. Mulargia [a], M.M. Obertino [a,b], G. Ortona [a], L. Pacher [a,b], N. Pastrone [a], M. Pelliccioni [a], M. Ruspa [a,c], K. Shchelina [a], F. Siviero [a,b], V. Sola [a,b], A. Solano [a,b], D. Soldi [a,b], A. Staiano [a], M. Tornago [a,b], D. Trocino [a], G. Umoret [a,b], A. Vagnerini [a,b]

[a] *INFN Sezione di Torino, Torino, Italy*
[b] *Università di Torino, Torino, Italy*
[c] *Università del Piemonte Orientale, Novara, Italy*

S. Belforte [a], V. Candelise [a,b], M. Casarsa [a], F. Cossutti [a], G. Della Ricca [a,b], G. Sorrentino [a,b]

[a] *INFN Sezione di Trieste, Trieste, Italy*
[b] *Università di Trieste, Trieste, Italy*

S. Dogra, C. Huh, B. Kim, D.H. Kim, G.N. Kim, J. Kim, J. Lee, S.W. Lee, C.S. Moon, Y.D. Oh, S.I. Pak, M.S. Ryu, S. Sekmen, Y.C. Yang

Kyungpook National University, Daegu, Korea

H. Kim, D.H. Moon

Chonnam National University, Institute for Universe and Elementary Particles, Kwangju, Korea

E. Asilar, T.J. Kim, J. Park

Hanyang University, Seoul, Korea

S. Choi, S. Han, B. Hong, K. Lee, K.S. Lee, J. Lim, J. Park, S.K. Park, J. Yoo

Korea University, Seoul, Korea

J. Goh

Kyung Hee University, Department of Physics, Seoul, Korea

H.S. Kim, Y. Kim, S. Lee

Sejong University, Seoul, Korea

J. Almond, J.H. Bhyun, J. Choi, S. Jeon, J. Kim, J.S. Kim, S. Ko, H. Kwon, H. Lee, S. Lee, B.H. Oh, S.B. Oh, H. Seo, U.K. Yang, I. Yoon

Seoul National University, Seoul, Korea

W. Jang, D.Y. Kang, Y. Kang, D. Kim, S. Kim, B. Ko, J.S.H. Lee, Y. Lee, J.A. Merlin, I.C. Park, Y. Roh, D. Song, I.J. Watson, S. Yang

University of Seoul, Seoul, Korea

S. Ha, H.D. Yoo

Yonsei University, Department of Physics, Seoul, Korea

M. Choi, M.R. Kim, H. Lee, Y. Lee, Y. Lee, I. Yu

Sungkyunkwan University, Suwon, Korea

T. Beyrouthy, Y. Maghrbi

College of Engineering and Technology, American University of the Middle East (AUM), Dasman, Kuwait

K. Dreimanis, G. Pikurs, A. Potrebko, M. Seidel, V. Veckalns

Riga Technical University, Riga, Latvia

M. Ambrozas, A. Carvalho Antunes De Oliveira, A. Juodagalvis, A. Rinkevicius, G. Tamulaitis

Vilnius University, Vilnius, Lithuania

N. Bin Norjoharuddeen, S.Y. Hoh [55], I. Yusuff [55], Z. Zolkapli

National Centre for Particle Physics, Universiti Malaya, Kuala Lumpur, Malaysia

J.F. Benitez, A. Castaneda Hernandez, H.A. Encinas Acosta, L.G. Gallegos Maríñez, M. León Coello, J.A. Murillo Quijada, A. Sehrawat, L. Valencia Palomo

Universidad de Sonora (UNISON), Hermosillo, Mexico

G. Ayala, H. Castilla-Valdez, I. Heredia-De La Cruz [56], R. Lopez-Fernandez, C.A. Mondragon Herrera, D.A. Perez Navarro, A. Sánchez Hernández

Centro de Investigacion y de Estudios Avanzados del IPN, Mexico City, Mexico

C. Oropeza Barrera, F. Vazquez Valencia

Universidad Iberoamericana, Mexico City, Mexico

I. Pedraza, H.A. Salazar Ibarguen, C. Uribe Estrada

Benemerita Universidad Autonoma de Puebla, Puebla, Mexico

I. Bubanja, J. Mijuskovic [57], N. Raicevic

University of Montenegro, Podgorica, Montenegro

A. Ahmad, M.I. Asghar, A. Awais, M.I.M. Awan, M. Gul, H.R. Hoorani, W.A. Khan

National Centre for Physics, Quaid-I-Azam University, Islamabad, Pakistan

V. Avati, L. Grzanka, M. Malawski

AGH University of Science and Technology Faculty of Computer Science, Electronics and Telecommunications, Krakow, Poland

H. Bialkowska, M. Bluj, B. Boimska, M. Górski, M. Kazana, M. Szleper, P. Zalewski

National Centre for Nuclear Research, Swierk, Poland

K. Bunkowski, K. Doroba, A. Kalinowski, M. Konecki, J. Krolikowski

Institute of Experimental Physics, Faculty of Physics, University of Warsaw, Warsaw, Poland

M. Araujo, P. Bargassa, D. Bastos, A. Boletti, P. Faccioli, M. Gallinaro, J. Hollar, N. Leonardo, T. Niknejad, M. Pisano, J. Seixas, J. Varela

Laboratório de Instrumentação e Física Experimental de Partículas, Lisboa, Portugal

P. Adzic [58], M. Dordevic, P. Milenovic, J. Milosevic

VINCA Institute of Nuclear Sciences, University of Belgrade, Belgrade, Serbia

M. Aguilar-Benitez, J. Alcaraz Maestre, M. Barrio Luna, Cristina F. Bedoya, C.A. Carrillo Montoya, M. Cepeda, M. Cerrada, N. Colino, B. De La Cruz, A. Delgado Peris, D. Fernández Del Val, J.P. Fernández Ramos, J. Flix, M.C. Fouz, O. Gonzalez Lopez, S. Goy Lopez, J.M. Hernandez, M.I. Josa, J. León Holgado, D. Moran, C. Perez Dengra, A. Pérez-Calero Yzquierdo, J. Puerta Pelayo, I. Redondo, D.D. Redondo Ferrero, L. Romero, S. Sánchez Navas, J. Sastre, L. Urda Gómez, J. Vazquez Escobar, C. Willmott

Centro de Investigaciones Energéticas Medioambientales y Tecnológicas (CIEMAT), Madrid, Spain

J.F. de Trocóniz

Universidad Autónoma de Madrid, Madrid, Spain

B. Alvarez Gonzalez, J. Cuevas, J. Fernandez Menendez, S. Folgueras, I. Gonzalez Caballero, J.R. González Fernández, E. Palencia Cortezon, C. Ramón Álvarez, V. Rodríguez Bouza, A. Soto Rodríguez, A. Trapote, C. Vico Villalba

Universidad de Oviedo, Instituto Universitario de Ciencias y Tecnologías Espaciales de Asturias (ICTEA), Oviedo, Spain

J.A. Brochero Cifuentes, I.J. Cabrillo, A. Calderon, J. Duarte Campderros, M. Fernandez, C. Fernandez Madrazo, A. García Alonso, G. Gomez, C. Lasaosa García, C. Martinez Rivero, P. Martinez Ruiz del Arbol, F. Matorras, P. Matorras Cuevas, J. Piedra Gomez, C. Prieels, L. Scodellaro, I. Vila, J.M. Vizan Garcia

Instituto de Física de Cantabria (IFCA), CSIC-Universidad de Cantabria, Santander, Spain

M.K. Jayananda, B. Kailasapathy [59], D.U.J. Sonnadara, D.D.C. Wickramarathna

University of Colombo, Colombo, Sri Lanka

W.G.D. Dharmaratna, K. Liyanage, N. Perera, N. Wickramage

University of Ruhuna, Department of Physics, Matara, Sri Lanka

D. Abbaneo, J. Alimena, E. Auffray, G. Auzinger, J. Baechler, P. Baillon [†], D. Barney, J. Bendavid, M. Bianco, B. Bilin, A. Bocci, E. Brondolin, C. Caillol, T. Camporesi, G. Cerminara, N. Chernyavskaya, S.S. Chhibra, S. Choudhury, M. Cipriani, L. Cristella, D. d'Enterria, A. Dabrowski, A. David, A. De Roeck, M.M. Defranchis, M. Deile, M. Dobson, M. Dünser, N. Dupont, F. Fallavollita [60], A. Florent, L. Forthomme, G. Franzoni, W. Funk, S. Ghosh, S. Giani, D. Gigi, K. Gill, F. Glege, L. Gouskos, E. Govorkova, M. Haranko, J. Hegeman, V. Innocente, T. James, P. Janot, J. Kaspar, J. Kieseler, N. Kratochwil, S. Laurila, P. Lecoq, E. Leutgeb, C. Lourenço, B. Maier, L. Malgeri, M. Mannelli, A.C. Marini, F. Meijers, S. Mersi, E. Meschi, F. Moortgat, M. Mulders, S. Orfanelli, L. Orsini, F. Pantaleo, E. Perez, M. Peruzzi, A. Petrilli, G. Petrucciani, A. Pfeiffer, M. Pierini, D. Piparo, M. Pitt, H. Qu, T. Quast, D. Rabady, A. Racz, G. Reales Gutiérrez, M. Rovere, H. Sakulin, J. Salfeld-Nebgen, S. Scarfi, M. Selvaggi, A. Sharma, P. Silva, P. Sphicas [61], A.G. Stahl Leiton, S. Summers, K. Tatar, D. Treille, P. Tropea, A. Tsirou, J. Wanczyk [62], K.A. Wozniak, W.D. Zeuner

CERN, European Organization for Nuclear Research, Geneva, Switzerland

L. Caminada [63], A. Ebrahimi, W. Erdmann, R. Horisberger, Q. Ingram, H.C. Kaestli, D. Kotlinski, C. Lange, M. Missiroli [63], L. Noehte [63], T. Rohe

Paul Scherrer Institut, Villigen, Switzerland

T.K. Aarrestad, K. Androsov [62], M. Backhaus, P. Berger, A. Calandri, K. Datta, A. De Cosa, G. Dissertori, M. Dittmar, M. Donegà, F. Eble, M. Galli, K. Gedia, F. Glessgen, T.A. Gómez Espinosa, C. Grab, D. Hits, W. Lustermann, A.-M. Lyon, R.A. Manzoni, L. Marchese, C. Martin Perez, A. Mascellani [62], F. Nessi-Tedaldi, J. Niedziela, F. Pauss, V. Perovic, S. Pigazzini, M.G. Ratti, M. Reichmann, C. Reissel, T. Reitenspiess, B. Ristic, F. Riti, D. Ruini, D.A. Sanz Becerra, J. Steggemann [62], D. Valsecchi [27], R. Wallny

ETH Zurich - Institute for Particle Physics and Astrophysics (IPA), Zurich, Switzerland

C. Amsler [64], P. Bärtschi, C. Botta, D. Brzhechko, M.F. Canelli, K. Cormier, A. De Wit, R. Del Burgo, J.K. Heikkilä, M. Huwiler, W. Jin, A. Jofrehei, B. Kilminster, S. Leontsinis, S.P. Liechti, A. Macchiolo, P. Meiring, V.M. Mikuni, U. Molinatti, I. Neutelings, A. Reimers, P. Robmann, S. Sanchez Cruz, K. Schweiger, M. Senger, Y. Takahashi

Universität Zürich, Zurich, Switzerland

C. Adloff [65], C.M. Kuo, W. Lin, P.K. Rout, P.C. Tiwari [39], S.S. Yu

National Central University, Chung-Li, Taiwan

L. Ceard, Y. Chao, K.F. Chen, P.s. Chen, H. Cheng, W.-S. Hou, R. Khurana, G. Kole, Y.y. Li, R.-S. Lu, E. Paganis, A. Psallidas, A. Steen, H.y. Wu, E. Yazgan

National Taiwan University (NTU), Taipei, Taiwan

C. Asawatangtrakuldee, N. Srimanobhas, V. Wachirapusitanand

Chulalongkorn University, Faculty of Science, Department of Physics, Bangkok, Thailand

D. Agyel, F. Boran, Z.S. Demiroglu, F. Dolek, I. Dumanoglu [66], E. Eskut, Y. Guler [67], E. Gurpinar Guler [67], C. Isik, O. Kara, A. Kayis Topaksu, U. Kiminsu, G. Onengut, K. Ozdemir [68], A. Polatoz, A.E. Simsek, B. Tali [69], U.G. Tok, S. Turkcapar, E. Uslan, I.S. Zorbakir

Çukurova University, Physics Department, Science and Art Faculty, Adana, Turkey

G. Karapinar [70], K. Ocalan [71], M. Yalvac [72]

Middle East Technical University, Physics Department, Ankara, Turkey

B. Akgun, I.O. Atakisi, E. Gülmez, M. Kaya [73], O. Kaya [74], S. Tekten [75]

Bogazici University, Istanbul, Turkey

A. Cakir, K. Cankocak [66], Y. Komurcu, S. Sen [66]

Istanbul Technical University, Istanbul, Turkey

O. Aydilek, S. Cerci [69], B. Hacisahinoglu, I. Hos [76], B. Isildak [77], B. Kaynak, S. Ozkorucuklu, C. Simsek, D. Sunar Cerci [69]

Istanbul University, Istanbul, Turkey

B. Grynyov

Institute for Scintillation Materials of National Academy of Science of Ukraine, Kharkiv, Ukraine

L. Levchuk

National Science Centre, Kharkiv Institute of Physics and Technology, Kharkiv, Ukraine

D. Anthony, J.J. Brooke, A. Bundock, E. Clement, D. Cussans, H. Flacher, M. Glowacki, J. Goldstein, H.F. Heath, L. Kreczko, B. Krikler, S. Paramesvaran, S. Seif El Nasr-Storey, V.J. Smith, N. Stylianou [78], K. Walkingshaw Pass, R. White

University of Bristol, Bristol, United Kingdom

A.H. Ball, K.W. Bell, A. Belyaev [79], C. Brew, R.M. Brown, D.J.A. Cockerill, C. Cooke, K.V. Ellis, K. Harder, S. Harper, M.-L. Holmberg [80], Sh. Jain, J. Linacre, K. Manolopoulos, D.M. Newbold, E. Olaiya, D. Petyt, T. Reis, G. Salvi, T. Schuh, C.H. Shepherd-Themistocleous, I.R. Tomalin, T. Williams

Rutherford Appleton Laboratory, Didcot, United Kingdom

R. Bainbridge, P. Bloch, S. Bonomally, J. Borg, C.E. Brown, O. Buchmuller, V. Cacchio, V. Cepaitis, G.S. Chahal [81], D. Colling, J.S. Dancu, P. Dauncey, G. Davies, J. Davies, M. Della Negra, S. Fayer, G. Fedi, G. Hall, M.H. Hassanshahi, A. Howard, G. Iles, J. Langford, L. Lyons, A.-M. Magnan, S. Malik, A. Martelli, M. Mieskolainen, D.G. Monk, J. Nash [82], M. Pesaresi, B.C. Radburn-Smith, D.M. Raymond, A. Richards, A. Rose, E. Scott, C. Seez, R. Shukla, A. Tapper, K. Uchida, G.P. Uttley, L.H. Vage, T. Virdee [27], M. Vojinovic, N. Wardle, S.N. Webb, D. Winterbottom

Imperial College, London, United Kingdom

K. Coldham, J.E. Cole, A. Khan, P. Kyberd, I.D. Reid

Brunel University, Uxbridge, United Kingdom

S. Abdullin, A. Brinkerhoff, B. Caraway, J. Dittmann, K. Hatakeyama, A.R. Kanuganti, B. McMaster, M. Saunders, S. Sawant, C. Sutantawibul, M. Toms, J. Wilson

Baylor University, Waco, TX, USA

R. Bartek, A. Dominguez, R. Uniyal, A.M. Vargas Hernandez

Catholic University of America, Washington, DC, USA

S.I. Cooper, D. Di Croce, S.V. Gleyzer, C. Henderson, C.U. Perez, P. Rumerio [83], C. West

The University of Alabama, Tuscaloosa, AL, USA

A. Akpinar, A. Albert, D. Arcaro, C. Cosby, Z. Demiragli, C. Erice, E. Fontanesi, D. Gastler, S. May, J. Rohlf, K. Salyer, D. Sperka, D. Spitzbart, I. Suarez, A. Tsatsos, S. Yuan

Boston University, Boston, MA, USA

G. Benelli, B. Burkle, X. Coubez [22], D. Cutts, M. Hadley, U. Heintz, J.M. Hogan [84], T. Kwon, G. Landsberg, K.T. Lau, D. Li, J. Luo, M. Narain, N. Pervan, S. Sagir [85], F. Simpson, E. Usai, W.Y. Wong, X. Yan, D. Yu, W. Zhang

Brown University, Providence, RI, USA

J. Bonilla, C. Brainerd, R. Breedon, M. Calderon De La Barca Sanchez, M. Chertok, J. Conway, P.T. Cox, R. Erbacher, G. Haza, F. Jensen, O. Kukral, G. Mocellin, M. Mulhearn, D. Pellett, B. Regnery, Y. Yao, F. Zhang

University of California, Davis, Davis, CA, USA

M. Bachtis, R. Cousins, A. Datta, D. Hamilton, J. Hauser, M. Ignatenko, M.A. Iqbal, T. Lam, E. Manca, W.A. Nash, D. Saltzberg, B. Stone, V. Valuev

University of California, Los Angeles, CA, USA

R. Clare, J.W. Gary, M. Gordon, G. Hanson, G. Karapostoli, O.R. Long, N. Manganelli, W. Si, S. Wimpenny

University of California, Riverside, Riverside, CA, USA

J.G. Branson, P. Chang, S. Cittolin, S. Cooperstein, D. Diaz, J. Duarte, R. Gerosa, L. Giannini, J. Guiang, R. Kansal, V. Krutelyov, R. Lee, J. Letts, M. Masciovecchio, F. Mokhtar, M. Pieri, B.V. Sathia Narayanan, V. Sharma, M. Tadel, E. Vourliotis, F. Würthwein, Y. Xiang, A. Yagil

University of California, San Diego, La Jolla, CA, USA

N. Amin, C. Campagnari, M. Citron, G. Collura, A. Dorsett, V. Dutta, J. Incandela, M. Kilpatrick, J. Kim, A.J. Li, P. Masterson, H. Mei, M. Oshiro, M. Quinnan, J. Richman, U. Sarica, R. Schmitz, F. Setti, J. Sheplock, P. Siddireddy, D. Stuart, S. Wang

University of California, Santa Barbara - Department of Physics, Santa Barbara, CA, USA

A. Bornheim, O. Cerri, I. Dutta, A. Latorre, J.M. Lawhorn, J. Mao, H.B. Newman, T.Q. Nguyen, M. Spiropulu, J.R. Vlimant, C. Wang, S. Xie, R.Y. Zhu

California Institute of Technology, Pasadena, CA, USA

J. Alison, S. An, M.B. Andrews, P. Bryant, T. Ferguson, A. Harilal, C. Liu, T. Mudholkar, S. Murthy, M. Paulini, A. Roberts, A. Sanchez, W. Terrill

Carnegie Mellon University, Pittsburgh, PA, USA

J.P. Cumalat, W.T. Ford, A. Hassani, G. Karathanasis, E. MacDonald, F. Marini, A. Perloff, C. Savard, N. Schonbeck, K. Stenson, K.A. Ulmer, S.R. Wagner, N. Zipper

University of Colorado Boulder, Boulder, CO, USA

J. Alexander, S. Bright-Thonney, X. Chen, D.J. Cranshaw, J. Fan, X. Fan, D. Gadkari, S. Hogan, J. Monroy, J.R. Patterson, D. Quach, J. Reichert, M. Reid, A. Ryd, J. Thom, P. Wittich, R. Zou

Cornell University, Ithaca, NY, USA

M. Albrow, M. Alyari, G. Apollinari, A. Apresyan, L.A.T. Bauerdick, D. Berry, J. Berryhill, P.C. Bhat, K. Burkett, J.N. Butler, A. Canepa, G.B. Cerati, H.W.K. Cheung, F. Chlebana, K.F. Di Petrillo, J. Dickinson, V.D. Elvira, Y. Feng, J. Freeman, A. Gandrakota, Z. Gecse, L. Gray, D. Green, S. Grünendahl, D. Guerrero, O. Gutsche, R.M. Harris, R. Heller, T.C. Herwig, J. Hirschauer, L. Horyn, B. Jayatilaka, S. Jindariani, M. Johnson, U. Joshi, T. Klijnsma, B. Klima, K.H.M. Kwok, S. Lammel, D. Lincoln, R. Lipton, T. Liu, C. Madrid, K. Maeshima, C. Mantilla, D. Mason, P. McBride, P. Merkel, S. Mrenna, S. Nahn, J. Ngadiuba, D. Noonan, V. Papadimitriou, N. Pastika, K. Pedro, C. Pena [86], F. Ravera, A. Reinsvold Hall [87], L. Ristori, E. Sexton-Kennedy, N. Smith, A. Soha, L. Spiegel, J. Strait, L. Taylor, S. Tkaczyk, N.V. Tran, L. Uplegger, E.W. Vaandering, I. Zoi

Fermi National Accelerator Laboratory, Batavia, IL, USA

P. Avery, D. Bourilkov, L. Cadamuro, V. Cherepanov, R.D. Field, E. Koenig, J. Konigsberg, A. Korytov, E. Kuznetsova, K.H. Lo, K. Matchev, N. Menendez, G. Mitselmakher, A. Muthirakalayil Madhu, N. Rawal, D. Rosenzweig, S. Rosenzweig, K. Shi, J. Wang, Z. Wu

University of Florida, Gainesville, FL, USA

T. Adams, A. Askew, N. Bower, R. Habibullah, V. Hagopian, T. Kolberg, G. Martinez, H. Prosper, O. Viazlo, M. Wulansatiti, R. Yohay, J. Zhang

Florida State University, Tallahassee, FL, USA

M.M. Baarmand, S. Butalla, T. Elkafrawy [53], M. Hohlmann, R. Kumar Verma, M. Rahmani, F. Yumiceva

Florida Institute of Technology, Melbourne, FL, USA

M.R. Adams, H. Becerril Gonzalez, R. Cavanaugh, S. Dittmer, O. Evdokimov, C.E. Gerber, D.J. Hofman, D.S. Lemos, A.H. Merrit, C. Mills, G. Oh, T. Roy, S. Rudrabhatla, M.B. Tonjes, N. Varelas, X. Wang, Z. Ye, J. Yoo

University of Illinois at Chicago (UIC), Chicago, IL, USA

M. Alhusseini, K. Dilsiz [88], L. Emediato, G. Karaman, O.K. Köseyan, J.-P. Merlo, A. Mestvirishvili [89], J. Nachtman, O. Neogi, H. Ogul [90], Y. Onel, A. Penzo, C. Snyder, E. Tiras [91]

The University of Iowa, Iowa City, IA, USA

O. Amram, B. Blumenfeld, L. Corcodilos, J. Davis, A.V. Gritsan, S. Kyriacou, P. Maksimovic, J. Roskes, S. Sekhar, M. Swartz, T.Á. Vámi

Johns Hopkins University, Baltimore, MD, USA

A. Abreu, L.F. Alcerro Alcerro, J. Anguiano, P. Baringer, A. Bean, Z. Flowers, T. Isidori, J. King, G. Krintiras, M. Lazarovits, C. Le Mahieu, C. Lindsey, J. Marquez, N. Minafra, M. Murray, M. Nickel, C. Rogan, C. Royon, R. Salvatico, S. Sanders, C. Smith, Q. Wang, G. Wilson

The University of Kansas, Lawrence, KS, USA

B. Allmond, S. Duric, A. Ivanov, K. Kaadze, A. Kalogeropoulos, D. Kim, Y. Maravin, T. Mitchell, A. Modak, K. Nam, D. Roy

Kansas State University, Manhattan, KS, USA

F. Rebassoo, D. Wright

Lawrence Livermore National Laboratory, Livermore, CA, USA

E. Adams, A. Baden, O. Baron, A. Belloni, A. Bethani, S.C. Eno, N.J. Hadley, S. Jabeen, R.G. Kellogg, T. Koeth, Y. Lai, S. Lascio, A.C. Mignerey, S. Nabili, C. Palmer, C. Papageorgakis, L. Wang, K. Wong

University of Maryland, College Park, MD, USA

D. Abercrombie, W. Busza, I.A. Cali, Y. Chen, M. D'Alfonso, J. Eysermans, C. Freer, G. Gomez-Ceballos, M. Goncharov, P. Harris, M. Hu, D. Kovalskyi, J. Krupa, Y.-J. Lee, K. Long, C. Mironov, C. Paus, D. Rankin, C. Roland, G. Roland, Z. Shi, G.S.F. Stephans, J. Wang, Z. Wang, B. Wyslouch, T.J. Yang

Massachusetts Institute of Technology, Cambridge, MA, USA

R.M. Chatterjee, B. Crossman, J. Hiltbrand, B.M. Joshi, C. Kapsiak, M. Krohn, Y. Kubota, J. Mans, M. Revering, R. Rusack, R. Saradhy, N. Schroeder, N. Strobbe, M.A. Wadud

University of Minnesota, Minneapolis, MN, USA

L.M. Cremaldi

University of Mississippi, Oxford, MS, USA

K. Bloom, M. Bryson, D.R. Claes, C. Fangmeier, L. Finco, F. Golf, C. Joo, R. Kamalieddin, I. Kravchenko, I. Reed, J.E. Siado, G.R. Snow [†], W. Tabb, A. Wightman, F. Yan, A.G. Zecchinelli

University of Nebraska-Lincoln, Lincoln, NE, USA

G. Agarwal, H. Bandyopadhyay, L. Hay, I. Iashvili, A. Kharchilava, C. McLean, M. Morris, D. Nguyen, J. Pekkanen, S. Rappoccio, A. Williams

State University of New York at Buffalo, Buffalo, NY, USA

G. Alverson, E. Barberis, Y. Haddad, Y. Han, A. Krishna, J. Li, J. Lidrych, G. Madigan, B. Marzocchi, D.M. Morse, V. Nguyen, T. Orimoto, A. Parker, L. Skinnari, A. Tishelman-Charny, T. Wamorkar, B. Wang, A. Wisecarver, D. Wood

Northeastern University, Boston, MA, USA

S. Bhattacharya, J. Bueghly, Z. Chen, A. Gilbert, K.A. Hahn, Y. Liu, N. Odell, M.H. Schmitt, M. Velasco

Northwestern University, Evanston, IL, USA

R. Band, R. Bucci, M. Cremonesi, A. Das, R. Goldouzian, M. Hildreth, K. Hurtado Anampa, C. Jessop, K. Lannon, J. Lawrence, N. Loukas, L. Lutton, J. Mariano, N. Marinelli, I. Mcalister, T. McCauley, C. Mcgrady, K. Mohrman, C. Moore, Y. Musienko [12], R. Ruchti, A. Townsend, M. Wayne, H. Yockey, M. Zarucki, L. Zygala

University of Notre Dame, Notre Dame, IN, USA

B. Bylsma, M. Carrigan, L.S. Durkin, C. Hill, M. Joyce, A. Lesauvage, M. Nunez Ornelas, K. Wei, B.L. Winer, B.R. Yates

The Ohio State University, Columbus, OH, USA

F.M. Addesa, P. Das, G. Dezoort, P. Elmer, A. Frankenthal, B. Greenberg, N. Haubrich, S. Higginbotham, G. Kopp, S. Kwan, D. Lange, D. Marlow, I. Ojalvo, J. Olsen, D. Stickland, C. Tully

Princeton University, Princeton, NJ, USA

S. Malik, S. Norberg

University of Puerto Rico, Mayaguez, PR, USA

A.S. Bakshi, V.E. Barnes, R. Chawla, S. Das, L. Gutay, M. Jones, A.W. Jung, D. Kondratyev, A.M. Koshy, M. Liu, G. Negro, N. Neumeister, G. Paspalaki, S. Piperov, A. Purohit, J.F. Schulte, M. Stojanovic, J. Thieman, F. Wang, R. Xiao, W. Xie

Purdue University, West Lafayette, IN, USA

J. Dolen, N. Parashar

Purdue University Northwest, Hammond, IN, USA

D. Acosta, A. Baty, T. Carnahan, S. Dildick, K.M. Ecklund, P.J. Fernández Manteca, S. Freed, P. Gardner, F.J.M. Geurts, A. Kumar, W. Li, B.P. Padley, R. Redjimi, J. Rotter, S. Yang, E. Yigitbasi, Y. Zhang

Rice University, Houston, TX, USA

A. Bodek, P. de Barbaro, R. Demina, J.L. Dulemba, C. Fallon, M. Galanti, A. Garcia-Bellido, O. Hindrichs, A. Khukhunaishvili, P. Parygin, E. Popova, E. Ranken, R. Taus, G.P. Van Onsem

University of Rochester, Rochester, NY, USA

K. Goulianos

The Rockefeller University, New York, NY, USA

B. Chiarito, J.P. Chou, Y. Gershtein, E. Halkiadakis, A. Hart, M. Heindl, D. Jaroslawski, O. Karacheban [25], I. Laflotte, A. Lath, R. Montalvo, K. Nash, M. Osherson, H. Routray, S. Salur, S. Schnetzer, S. Somalwar, R. Stone, S.A. Thayil, S. Thomas, H. Wang

Rutgers, The State University of New Jersey, Piscataway, NJ, USA

H. Acharya, A.G. Delannoy, S. Fiorendi, T. Holmes, E. Nibigira, S. Spanier

University of Tennessee, Knoxville, TN, USA

O. Bouhali [92], M. Dalchenko, A. Delgado, R. Eusebi, J. Gilmore, T. Huang, T. Kamon [93], H. Kim, S. Luo, S. Malhotra, R. Mueller, D. Overton, D. Rathjens, A. Safonov

Texas A&M University, College Station, TX, USA

N. Akchurin, J. Damgov, V. Hegde, K. Lamichhane, S.W. Lee, T. Mengke, S. Muthumuni, T. Peltola, I. Volobouev, A. Whitbeck

Texas Tech University, Lubbock, TX, USA

E. Appelt, S. Greene, A. Gurrola, W. Johns, A. Melo, F. Romeo, P. Sheldon, S. Tuo, J. Velkovska, J. Viinikainen

Vanderbilt University, Nashville, TN, USA

B. Cardwell, B. Cox, G. Cummings, J. Hakala, R. Hirosky, A. Ledovskoy, A. Li, C. Neu, C.E. Perez Lara, B. Tannenwald

University of Virginia, Charlottesville, VA, USA

P.E. Karchin, N. Poudyal

Wayne State University, Detroit, MI, USA

S. Banerjee, K. Black, T. Bose, S. Dasu, I. De Bruyn, P. Everaerts, C. Galloni, H. He, M. Herndon, A. Herve, C.K. Koraka, A. Lanaro, A. Loeliger, R. Loveless, J. Madhusudanan Sreekala, A. Mallampalli, A. Mohammadi, S. Mondal, G. Parida, D. Pinna, A. Savin, V. Shang, V. Sharma, W.H. Smith, D. Teague, H.F. Tsoi, W. Vetens

University of Wisconsin - Madison, Madison, WI, USA

S. Afanasiev, V. Andreev, Yu. Andreev, T. Aushev, M. Azarkin, A. Babaev, A. Belyaev, V. Blinov [94], E. Boos, V. Borshch, D. Budkouski, V. Chekhovsky, R. Chistov [94], M. Danilov [94], A. Dermenev, T. Dimova [94], I. Dremin, M. Dubinin [86], L. Dudko, V. Epshteyn, A. Ershov, G. Gavrilov, V. Gavrilov, S. Gninenko, V. Golovtcov, N. Golubev, I. Golutvin, I. Gorbunov, A. Gribushin, Y. Ivanov, V. Kachanov, L. Kardapoltsev [94], V. Karjavine, A. Karneyeu, V. Kim [94], M. Kirakosyan, D. Kirpichnikov, M. Kirsanov, V. Klyukhin, O. Kodolova [95], D. Konstantinov, V. Korenkov, A. Kozyrev [94], N. Krasnikov, A. Lanev, P. Levchenko, A. Litomin, N. Lychkovskaya, V. Makarenko, A. Malakhov, V. Matveev [94], V. Murzin, A. Nikitenko [96], S. Obraztsov, I. Ovtin [94], V. Palichik, V. Perelygin, S. Petrushanko, S. Polikarpov [94], V. Popov, O. Radchenko [94], M. Savina, V. Savrin, D. Selivanova, V. Shalaev, S. Shmatov, S. Shulha, Y. Skovpen [94], S. Slabospitskii, V. Smirnov, A. Snigirev, D. Sosnov, V. Sulimov, E. Tcherniaev, A. Terkulov, O. Teryaev, I. Tlisova, A. Toropin, L. Uvarov, A. Uzunian, E. Vlasov, A. Vorobyev, N. Voytishin, B.S. Yuldashev [97], A. Zarubin, I. Zhizhin, A. Zhokin

Authors affiliated with an institute or an international laboratory covered by a cooperation agreement with CERN

† Deceased.
[1] Also at Yerevan State University, Yerevan, Armenia.
[2] Also at TU Wien, Vienna, Austria.
[3] Also at Institute of Basic and Applied Sciences, Faculty of Engineering, Arab Academy for Science, Technology and Maritime Transport, Alexandria, Egypt.
[4] Also at Université Libre de Bruxelles, Bruxelles, Belgium.
[5] Also at Universidade Estadual de Campinas, Campinas, Brazil.
[6] Also at Federal University of Rio Grande do Sul, Porto Alegre, Brazil.
[7] Also at UFMS, Nova Andradina, Brazil.
[8] Also at University of Chinese Academy of Sciences, Beijing, China.
[9] Also at Nanjing Normal University Department of Physics, Nanjing, China.
[10] Now at The University of Iowa, Iowa City, Iowa, USA.
[11] Also at University of Chinese Academy of Sciences, Beijing, China.
[12] Also at an institute or an international laboratory covered by a cooperation agreement with CERN.
[13] Now at British University in Egypt, Cairo, Egypt.
[14] Now at Cairo University, Cairo, Egypt.
[15] Also at Purdue University, West Lafayette, Indiana, USA.
[16] Also at Université de Haute Alsace, Mulhouse, France.
[17] Also at Department of Physics, Tsinghua University, Beijing, China.
[18] Also at Ilia State University, Tbilisi, Georgia.
[19] Also at The University of the State of Amazonas, Manaus, Brazil.
[20] Also at Erzincan Binali Yildirim University, Erzincan, Turkey.
[21] Also at University of Hamburg, Hamburg, Germany.
[22] Also at RWTH Aachen University, III. Physikalisches Institut A, Aachen, Germany.
[23] Also at Isfahan University of Technology, Isfahan, Iran.
[24] Also at Bergische University Wuppertal (BUW), Wuppertal, Germany.
[25] Also at Brandenburg University of Technology, Cottbus, Germany.
[26] Also at Forschungszentrum Jülich, Juelich, Germany.
[27] Also at CERN, European Organization for Nuclear Research, Geneva, Switzerland.
[28] Also at Physics Department, Faculty of Science, Assiut University, Assiut, Egypt.
[29] Also at Karoly Robert Campus, MATE Institute of Technology, Gyongyos, Hungary.
[30] Also at Wigner Research Centre for Physics, Budapest, Hungary.
[31] Also at Institute of Physics, University of Debrecen, Debrecen, Hungary.
[32] Also at Institute of Nuclear Research ATOMKI, Debrecen, Hungary.
[33] Now at Universitatea Babes-Bolyai - Facultatea de Fizica, Cluj-Napoca, Romania.

[34] Also at Faculty of Informatics, University of Debrecen, Debrecen, Hungary.
[35] Also at Punjab Agricultural University, Ludhiana, India.
[36] Also at UPES - University of Petroleum and Energy Studies, Dehradun, India.
[37] Also at University of Visva-Bharati, Santiniketan, India.
[38] Also at University of Hyderabad, Hyderabad, India.
[39] Also at Indian Institute of Science (IISc), Bangalore, India.
[40] Also at Indian Institute of Technology (IIT), Mumbai, India.
[41] Also at IIT Bhubaneswar, Bhubaneswar, India.
[42] Also at Institute of Physics, Bhubaneswar, India.
[43] Also at Deutsches Elektronen-Synchrotron, Hamburg, Germany.
[44] Also at Sharif University of Technology, Tehran, Iran.
[45] Also at Department of Physics, University of Science and Technology of Mazandaran, Behshahr, Iran.
[46] Also at Helwan University, Cairo, Egypt.
[47] Also at Italian National Agency for New Technologies, Energy and Sustainable Economic Development, Bologna, Italy.
[48] Also at Centro Siciliano di Fisica Nucleare e di Struttura Della Materia, Catania, Italy.
[49] Also at Università degli Studi Guglielmo Marconi, Roma, Italy.
[50] Also at Scuola Superiore Meridionale, Università di Napoli 'Federico II', Napoli, Italy.
[51] Also at Fermi National Accelerator Laboratory, Batavia, Illinois, USA.
[52] Also at Università di Napoli 'Federico II', Napoli, Italy.
[53] Also at Ain Shams University, Cairo, Egypt.
[54] Also at Consiglio Nazionale delle Ricerche - Istituto Officina dei Materiali, Perugia, Italy.
[55] Also at Department of Applied Physics, Faculty of Science and Technology, Universiti Kebangsaan Malaysia, Bangi, Malaysia.
[56] Also at Consejo Nacional de Ciencia y Tecnología, Mexico City, Mexico.
[57] Also at IRFU, CEA, Université Paris-Saclay, Gif-sur-Yvette, France.
[58] Also at Faculty of Physics, University of Belgrade, Belgrade, Serbia.
[59] Also at Trincomalee Campus, Eastern University, Sri Lanka, Nilaveli, Sri Lanka.
[60] Also at INFN Sezione di Pavia, Università di Pavia, Pavia, Italy.
[61] Also at National and Kapodistrian University of Athens, Athens, Greece.
[62] Also at Ecole Polytechnique Fédérale Lausanne, Lausanne, Switzerland.
[63] Also at Universität Zürich, Zurich, Switzerland.
[64] Also at Stefan Meyer Institute for Subatomic Physics, Vienna, Austria.
[65] Also at Laboratoire d'Annecy-le-Vieux de Physique des Particules, IN2P3-CNRS, Annecy-le-Vieux, France.
[66] Also at Near East University, Research Center of Experimental Health Science, Mersin, Turkey.
[67] Also at Konya Technical University, Konya, Turkey.
[68] Also at Izmir Bakircay University, Izmir, Turkey.
[69] Also at Adiyaman University, Adiyaman, Turkey.
[70] Also at Istanbul Gedik University, Istanbul, Turkey.
[71] Also at Necmettin Erbakan University, Konya, Turkey.
[72] Also at Bozok Universitetesi Rektörlügü, Yozgat, Turkey.
[73] Also at Marmara University, Istanbul, Turkey.
[74] Also at Milli Savunma University, Istanbul, Turkey.
[75] Also at Kafkas University, Kars, Turkey.
[76] Also at Istanbul University - Cerrahpasa, Faculty of Engineering, Istanbul, Turkey.
[77] Also at Yildiz Technical University, Istanbul, Turkey.
[78] Also at Vrije Universiteit Brussel, Brussel, Belgium.
[79] Also at School of Physics and Astronomy, University of Southampton, Southampton, United Kingdom.
[80] Also at University of Bristol, Bristol, United Kingdom.
[81] Also at IPPP Durham University, Durham, United Kingdom.
[82] Also at Monash University, Faculty of Science, Clayton, Australia.
[83] Also at Università di Torino, Torino, Italy.
[84] Also at Bethel University, St. Paul, Minnesota, USA.
[85] Also at Karamanoğlu Mehmetbey University, Karaman, Turkey.
[86] Also at California Institute of Technology, Pasadena, California, USA.
[87] Also at United States Naval Academy, Annapolis, Maryland, USA.
[88] Also at Bingol University, Bingol, Turkey.
[89] Also at Georgian Technical University, Tbilisi, Georgia.
[90] Also at Sinop University, Sinop, Turkey.
[91] Also at Erciyes University, Kayseri, Turkey.
[92] Also at Texas A&M University at Qatar, Doha, Qatar.
[93] Also at Kyungpook National University, Daegu, Korea.
[94] Also at another institute or international laboratory covered by a cooperation agreement with CERN.
[95] Also at Yerevan Physics Institute, Yerevan, Armenia.
[96] Also at Imperial College, London, United Kingdom.
[97] Also at Institute of Nuclear Physics of the Uzbekistan Academy of Sciences, Tashkent, Uzbekistan.